J. Fluid Mech. (1970), *vol.* 42, *part* 4, *pp.* 769–802
Printed in Great Britain

Characteristics of turbulent boundary layers at low Reynolds numbers with and without transpiration

By ROGER L. SIMPSON

Institute of Technology, Southern Methodist University, Dallas, Texas

(Received 14 April 1969 and in revised form 2 February 1970)

An extension to Coles's (1956) 'law of the wall–law of the wake' formulation for incompressible unblown boundary layers with momentum thickness Reynolds number $Re_\theta > 6000$ is made for $Re_\theta < 6000$. It is found that $\kappa = 0{\cdot}40$, the von Kármán constant for $Re_\theta > 6000$, is replaced by $\Omega = 0{\cdot}40\ (Re_\theta/6000)^{-\frac{1}{8}}$ for $Re_\theta < 6000$. Based upon the data of Simpson (1967) this formulation is extended to injection and undersucked ($d\theta/dx > 0$) flows in 'law of the wall' and 'velocity-defect' representations. This law of the wall for the logarithmic turbulent region and Reichardt's sublayer variation of ϵ_M/ν are used to obtain a continuous expression for ϵ_M/ν as a function of U^+, V_w^+, and Re_θ for the wall region. This expression is in reasonable agreement with the generated ϵ_M/ν blowing results and in less agreement with the unblown and suction results. Eddy viscosity and mixing length results confirm that $\epsilon_M/\delta^* U_\infty \propto \Omega^2$ and $l/\delta \propto \Omega$ for the outer region and that $\epsilon_M/\delta^* U_\infty$ and l/δ are substantially independent of blowing and moderate suction, as also reflected by the velocity defect representation for injection and suction.

1. Introduction

In recent years, considerable effort has been devoted to the study of incompressible turbulent boundary layers with uniform injection (blowing) or suction at the surface. Most of these investigations have logically begun with skin-friction and velocity profile correlations for the special case, the unblown flat plate. The experimental skin-friction coefficients for the flat plate with uniform injection are commonly presented in the form $(C_f/C_{f_0})_{Re_x}$ *vs.* b, the ratio $\rho_w V_w/\rho_\infty U_\infty$ ($\frac{1}{2}C_{f_0}$), where $\frac{1}{2}C_{f_0}$ is the zero injection case value. Here $\frac{1}{2}C_f$ is the friction factor defined by $\tau_w = \frac{1}{2}C_f(\rho_\infty U_\infty^2)$, τ is the shear stress, U is the velocity in the mainstream direction, V is the velocity perpendicular to the wall and subscripts w and ∞ indicate wall and free-stream conditions respectively. Several theories (Dorrance & Dore 1954; Rubesin 1954; Kendall *et al.* 1964; Torii, Nishiwaki & Hirata 1966; Stevenson 1964) show these experimental curves to be a function of Re_x. Simpson, Moffat & Kays (1969*a*) present $(C_f/C_{f_0})_{Re_\theta}$ *vs.* B, the ratio $\rho_w V_w/\rho_\infty U_\infty$ ($\frac{1}{2}C_f$), and have shown that this latter form of plotting transpiration data superimposes the data in the range $600 < Re_\theta < 6000$ for uniform and variable injection and suction.

As in the unblown case, all known investigations of transpired turbulent boundary layers present mean velocity profile correlations in terms of the local skin-friction coefficient. Many investigations present extensions of two commonly

accepted velocity profile functions for unblown layers, the law of the wall and Coles's (1956) law of the wake. However, it is no surprise that many of these extensions for blowing differ since the experimental skin-friction coefficient results of many investigators differ drastically for the same blowing condition (Simpson *et al.* 1969*a*).

For this reason Simpson (1967) and Simpson *et al.* (1969*a*) attempted to review the existing works, pointing out possible sources of experimental discrepancy described by the experimenters that could have produced different values of $\frac{1}{2}C_f$ for the same blowing condition. They found the uniform injection data of Simpson (1967) in substantial agreement with the results of Kendall (1959) and Stevenson (1964), Rotta (1966), and Kinney (1967) results from the Mickley–Davis (1957) data on a $(C_f/C_{f_0})_{Re_x}$ *vs.* b plot. In other investigations, acceptable unblown flat plate data were not reported; and, in others again, there were uncertainties in the blowing condition, or in the method used to evaluate $\frac{1}{2}C_f$ experimentally.

To add to the confusion, many investigators attempted to extend the unblown law of the wall and law of the wake to blown and sucked flows when $Re_\theta < 6000$, a range of Reynolds numbers in which Coles (1962) observed his law of the wake formulation to fail for unblown flows. Coles's observations were based on nearly 500 mean velocity profiles.

The present work has the broad threefold objective of: (i) extending Coles (1956) law of the wall–law of the wake formulation to unblown flat plate layers with $Re_\theta < 6000$; (ii) extending this formulation to the cases with blowing or suction; and (iii) extending eddy viscosity and Prandtl mixing length models to blowing and suction cases for use in turbulent boundary-layer prediction programs.

2. Experimental apparatus and the skin-friction results

The Stanford heat and mass transfer apparatus, as described in detail by Moffat & Kays (1967, 1968), was used in the experiments of Simpson (1967). The stagnation pressure probe instrumentation and fluid dynamic characteristics of the apparatus are discussed in detail by Simpson (1967) and Simpson *et al.* (1969). As a result of qualification tests, the boundary-layer flow was found to be essentially steady, two-dimensional, constant property, constant free-stream velocity turbulent flow over a smooth uniformly permeable flat plate. Simpson & Whitten (1968) calibrated Preston tubes with transpiration on this apparatus. Heat transfer and temperature profile data from this apparatus are reported by Moffat & Kays (1967, 1968), Whitten (1967), and Whitten, Kays & Moffat (1970). Simpson, Whitten & Moffat (1969*b*) used data from this apparatus to determine the effect of transpiration on the turbulent Prandtl number distribution in the boundary layer. The unblown flat plate skin-friction and heat transfer coefficient results agreed with accepted correlations while the mean velocity profiles were found to be 'normal' according to the criterion proposed by Coles (1962). The $\frac{1}{2}C_f$ results are discussed in considerable detail elsewhere (Simpson 1967; Simpson *et al.* 1969), but will be briefly reviewed here.

Two methods were used in determining the friction factor. One method used the momentum integral equation, differentiating a smooth fit of

$$Re_\theta - \int_0^{Re_x} \rho_w V_w / \rho_\infty U_\infty \, d(Re_\lambda) \; vs. \; Re_x$$

experimentally determined along the flow duct for each run. The second method used the viscous sublayer equation, relating experimental velocity points in the viscous sublayer to $\frac{1}{2}C$ in terms of the mass flux $\dot{m}''$ ($\equiv (\rho V)_w$) and $(\rho U)_\infty$. With the exception of two out of 95 velocity profile traverses, the values of $\frac{1}{2}C_f$ for a given traverse obtained by both methods agree within the uncertainty estimated at 20:1 odds. The $\frac{1}{2}C_f$ values used in all velocity profile correlations are 'best estimate' values presented and discussed by Simpson *et al.* (1969), and in general taken to be the momentum integral equation results.

The range of test conditions for the blowing and suction data of Simpson (1967) can be summarized as follows:

X-Reynolds number	$1{\cdot}3 \times 10^5$ to 2×10^6.
Blowing fraction, $m''/(\rho U)_\infty$	$-0{\cdot}00765$ to $0{\cdot}00958$.
Free-stream velocity, ft./sec	42 to 47.
Free-stream temperature, °F	64 to 90.

This, with the several injection and suction boundary conditions: (i) $\dot{m}''$ constant along the flow, (ii) $\dot{m}'' \propto X^{-0{\cdot}2}$ which results in a constant B flow, (iii) $\dot{m}'' \propto X$, and (iv) $\dot{m}'' \propto X^{-\frac{1}{2}}$. (By contrast, the data of Stevenson (1964), McQuaid (1966), Kendall (1959), Mickley, Smith & Fraser (1954, 1957), and all other distributed suction data, were obtained for $\dot{m}''$ nominally constant along the flow.)

3. Unblown flat plate

Coles (1956) presented the equation

$$U^+ = f(y^+) + g(\Pi, \eta), \tag{1}$$

where

$$f(y^+) = 1/\kappa \ln |y^+| + C$$

for the boundary layer on a flat plate in a uniform velocity stream, y is the distance along a line perpendicular to the plate, $\eta \equiv y/\delta$ (the dimensionless distance), $\delta \equiv y$ at $U/U_\infty = 0{\cdot}990$ (the boundary-layer thickness), Π is a parameter independent of X and y, $U^+ = U/U_\tau$ and $y^+ = yU_\tau/\nu$, where $U_\tau \equiv (\tau_w/\rho)^{\frac{1}{2}}$ (the shear velocity). Outside the sublayer, the velocity profile similarity can be expressed in terms of η by a relationship known as the velocity defect law:

$$\Gamma = \frac{U_\infty - U}{U_\tau} = F(\Pi, \eta), \tag{2}$$

which is a result of the logarithmic variation of f in (1). Based upon a survey of experimental data he presented

$$U^+ = \frac{1}{\kappa} \ln |y^+| + C + \frac{\Pi}{\kappa} \omega(\eta), \tag{3}$$

where $\kappa = 0{\cdot}40$, $C = 5{\cdot}1$, $\omega(\eta)$ is the Coles 'wake function'

$$\left(\omega(0) = 0, \quad \omega(1) = 2, \quad \text{and} \quad \int_0^1 \omega d\eta = 1\right),$$

and $\Pi = 0{\cdot}55$ for constant free-stream velocity flows. Hence, with $U \simeq U_\infty$ at $y = \delta$ in (3), (2) becomes

$$\frac{U_\infty - U}{U_\tau} = \frac{1}{\kappa}[-\ln|\eta| + \Pi(2 - \omega(\eta))] \tag{4}$$

for the velocity defect relation.

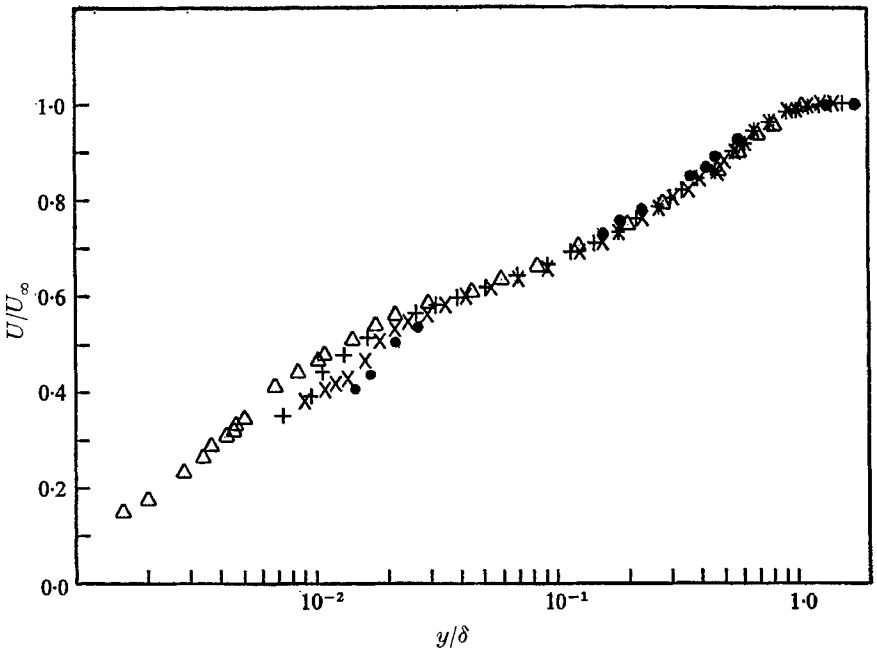

FIGURE 1. Zero injection data. Simpson (1967): ●, $Re_\theta = 1971$; ×, 3352; +, 4318. Klebanoff (1954): △, $Re_\theta = 7750$.

Coles (1962), upon examining nearly 500 unblown flat plate profiles, concluded that the velocity defect law, (4), does not apply when $Re_\theta < 6000$. Denoting the maximum value of $g(\Pi, \eta)$ as the *strength of the wake*, he found this parameter was sensitive to the history and environment of a particular flow, and was a well-defined function of Re_θ, making possible precise classification of boundary-layer data. Among the data he considered 'normal' or representative were the data of Wieghardt (1943), which he used in his 1956 work, and Klebanoff (1954). The data of Wieghardt are considered as good data by workers in the field, since it was the only adiabatic flat plate flow considered by the 1968 turbulent boundary layer prediction conference (Kline, Cockrell & Morkovin 1968).

In figures 1 and 2, the data show a definite U/U_∞ *vs.* η similarity independent of Re_θ in the region outside the sublayer for $1000 < Re_\theta < 6000$. As shown in figure 2, there is a departure from this outer region similarity at higher Reynolds

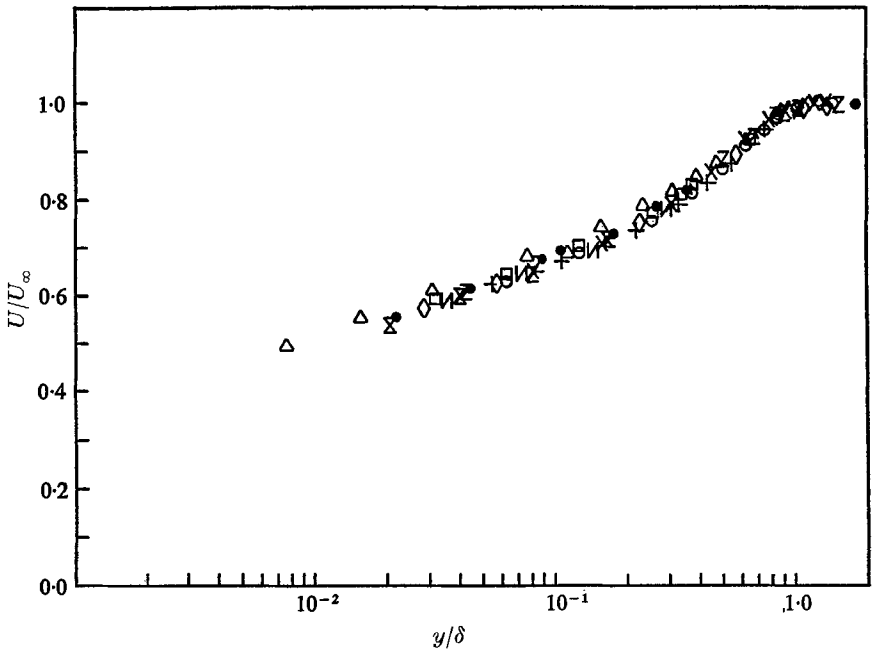

FIGURE 2. Unblown data of Wieghardt (1943). U_∞ = 33 m/sec.

●	Re_θ = 1036	+	2359	□	3813	⧖	6143
×	1527	z	2817	◇	4340	△	15439
○	1973	И	3380				

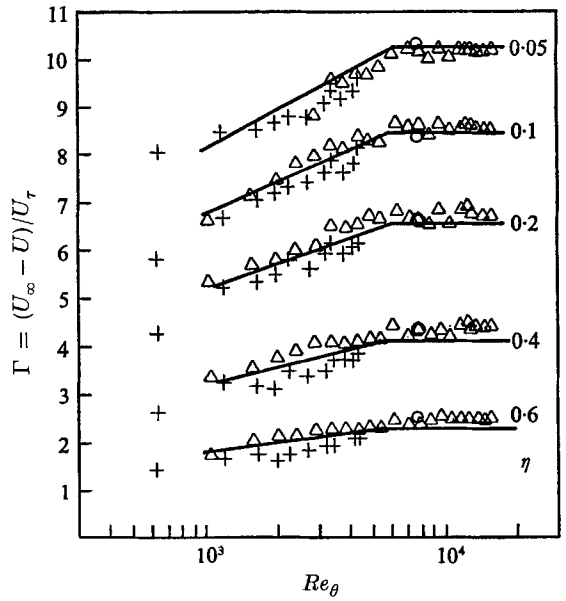

FIGURE 3. Unblown flat plate velocity defect representation (constant η). ○, Klebanoff (1954); △, Wieghardt (1943); +, Simpson (1967), —, equation (6), $\Omega = 0{\cdot}40\,(Re_\theta/6000)^{-\frac{1}{8}}$, $1000 < Re_\theta \leqslant 6000$, and $\Omega = 0{\cdot}40$, $Re_\theta > 6000$.

numbers. This similarity in the lower Reynolds number range is clearly in conflict with (4), since $U_\tau = U_\infty (\frac{1}{2}C_f)^{\frac{1}{2}} \sim Re_\theta^{-\frac{1}{8}}$. From another point of view, the quantity $(U_\infty - U)/U_\tau$ from these data was interpolated and plotted in figure 3 as a function of Re_θ for several constant values of η. The $\frac{1}{2}C_f$ values used were the values reported by the experimenters. Note that (4) only holds for Re_θ greater than about 6000.

In order to modify the velocity defect relation to account for the lower Reynolds number range similarity, it is sufficient to allow κ to vary proportional to $Re_\theta^{-\frac{1}{8}}$ or $(\frac{1}{2}C_f)^{\frac{1}{2}}$ for $Re_\theta < 6000$, while remaining fixed at higher Reynolds numbers. As shown in figure 3 this hypothesis fits the data well. (The departure of the $\eta = 0{\cdot}05$ data from this hypothesis for Re_θ less than 1000 is due to the data being in the viscous sublayer).

Millikan's argument for a logarithmic overlap region, in which the law of the wall and velocity defect relation hold simultaneously, remains unchanged if κ is allowed to vary with Re_θ. Consider the variable κ law of the wall,

$$U^+ = \frac{1}{\Omega(Re_\theta)} \ln |y^+| + C(Re_\theta) = q(y^+, Re_\theta), \tag{5}$$

and velocity defect relation

$$\Gamma = \frac{U_\infty - U}{U_\tau} = \frac{1}{\Omega(Re_\theta)} [-\ln |\eta| + \Pi(2 - \omega(\eta))] = E(\eta, \Pi, Re_\theta), \tag{6}$$

where $\Omega = 0{\cdot}40\,(Re_\theta/6000)^{-\frac{1}{8}}$ for $Re_\theta < 6000$ and $\Omega = \kappa = 0{\cdot}40$ for $Re_\theta > 6000$.

Hence

$$\frac{y}{U_\tau}\frac{\partial U}{\partial y} = y^+ \frac{\partial q}{\partial y^+} = \frac{1}{\Omega(Re_\theta)} \tag{7a}$$

from (5), and

$$\frac{y}{U_\tau}\frac{\partial U}{\partial y} = -\eta \frac{\partial E}{\partial \eta} = \frac{1}{\Omega(Re_\theta)} \tag{7b}$$

from (6) since $\omega'(\eta) \to 0$ in the region near the wall. Thus, both (5) and (6) remain valid and overlap in a region near the wall. As shown in figures 1 and 2, the outer edge of this logarithmic region is at about $\eta = 0{\cdot}1$.

To determine $C(Re_\theta)$ it is necessary to use the U/U_∞ *vs.* η similarity in the logarithmic region. Hence, using (5) for a given y/δ with $\frac{1}{2}C_f = 0{\cdot}0128\,Re_\theta^{-\frac{1}{4}}$ produces

$$C(Re_\theta) = Re_\theta^{\frac{1}{8}}[7{\cdot}90 - 0{\cdot}737 \ln |Re_\theta|]. \tag{8}$$

The result from this equation is shown on figure 4 for $Re_\theta = 1187$. The results using Coles (1956) constants in (5) are also shown for $Re_\theta > 6000$. Note that over the range $1000 < Re_\theta < 6000$ the logarithmic relation equation (5) pivots within the logarithmic region and near universal U^+ *vs.* y^+ similarity is obtained for $y/\delta < 0{\cdot}1$.

Thus, the idea of κ varying with Re_θ for $Re_\theta < 6000$ is plausible and consistent with experimental data.

4. Constant and slowly varying injection and suction cases

Turbulent velocity profiles for uniform free-stream velocity layers with constant or slowly varying wall-boundary conditions obey empirical similarity laws, generally described as a 'velocity defect' law in the outer region of the flow and a 'law of the wall' in the inner flow (Rotta 1962).

4.1. *The law of the wall*

In the region near the wall the flow is governed by the local conditions only and historical effects (the influence of the flow in the outer region) are contained in the shear velocity U_τ (Rotta 1962). (As discussed in § 3 for the unblown flat plate, the turbulent 'law of the wall' values Ω (Re_θ) and $C(Re_\theta)$ in the low Reynolds number range $1000 < Re_\theta < 6000$ are functions of Re_θ, and therefore contain some historical effects.) For constant property flow over a smooth uniformly permeable flat plate, the velocity U near the wall depends only on y, ν, V_w and U_τ, and Re_θ for the low Reynolds number range. From dimensional analysis, one obtains

$$U^+ = f(y^+, V_w^+, Re_\theta), \tag{9}$$

where $V_w^+ = V_w/U_\tau$. Equation (9) leads to what is known as the 'law of the wall with blowing and suction'.

We will consider two portions of the wall region. The portion nearer the wall is governed by a molecular viscosity and is known as the 'viscous sublayer', while the second portion is described by a turbulent mechanism and is known as the 'fully turbulent portion'. A third layer, the 'buffer layer' is sometimes assumed to exist between these two portions, but will not be discussed here.

Consider the X direction momentum equation with a purely laminar viscosity mechanism. Neglecting the X direction derivatives,

$$V_w \frac{dU}{dy} = \nu \frac{d^2U}{dy^2}. \tag{10}$$

Integrating (10) with the conditions $U = 0$ at $y = 0$ and

$$\nu(dU/dy) = U_\tau^2 = \tau_w/\rho \quad \text{at} \quad y = 0$$

produces (11) for the inner portion (Kendall 1959; Black & Sarnecki 1958; Stevenson 1963*a*):

$$U^+ = \frac{1}{V_w^+}[\exp\{V_w^+ y^+\} - 1]. \tag{11}$$

This equation is the viscous sublayer equation, which was used to obtain $\frac{1}{2}C_f$ by the viscous sublayer method.

Many investigators studying blowing and suction have used the Prandtl mixing length hypothesis to describe the turbulent portion. First, the X direction momentum equation is written, neglecting X derivatives:

$$V_w \frac{dU}{dy} = \frac{1}{\rho}\frac{d\tau}{dy}. \tag{12}$$

Solving (12) with the condition $\tau = \tau_w$ at $y = 0$ yields

$$\tau = \tau_w + \rho_w V_w U. \tag{13}$$

Using the mixing length hypothesis with the assumption that the mixing length is proportional to the distance from the wall results in

$$\frac{\tau_t}{\rho} = \left(\Omega y \frac{dU}{dy}\right)^2, \tag{14}$$

where Ω is independent of y. Equations (13) and (14) can be combined and integrated to produce

$$\phi = \frac{2}{V_w^+}[(1 + U^+ V_w^+)^{\frac{1}{2}} - (1 + U_a^+ V_w^+)^{\frac{1}{2}}] = \frac{1}{\Omega} \ln \left|\frac{y^+}{y_a^+}\right|, \tag{15}$$

where U_a^+, y_a^+, and Ω are in general functions of V_w^+ and Re_θ. For $V_w^+ = 0$, (15) reduces to the formula,

$$U^+ = (1/\Omega) \ln |y^+| - (1/\Omega) \ln |y_a^+| + U_a^+, \tag{16}$$

which is another form of (5).

Stevenson (1963*a*) presented an excellent summary of the work of the many investigators (Mickley *et al.* 1954; Black & Sarnecki 1958; Clark, Menkes & Libby 1955; Rubesin 1954; Dorrance & Dore 1954), who have obtained (15) in one form or another, assuming a constant Ω, although most of the data are in the low Reynolds number range. For fully turbulent flows with $V_w/U_\infty < 10^{-2}$, the value of Ω has been bound, in all studies, to be independent of V_w^+ (Stevenson 1963*a*). Black & Sarnecki (1958), in particular, argued that the mixing-length coefficient Ω should be independent of V_w, provided V_w is small compared to U in the region where (14) appears to hold. They demonstrated that the mean flow curvature near the wall, which was presumed to affect Ωy, is still small, as in the unblown case, for flows with V_w/U_∞ as high as 10^{-2}. In Simpson (1967), a constant value of $\Omega = 0{\cdot}44$ was used in (15) to fit Simpson's data. It is not surprising that this value fits the ϕ *vs.* y^+ data better *as a whole* than $\Omega = \kappa = 0{\cdot}40$, since nearly all the data of Simpson were in the low Reynolds number range $1000 < Re_\theta < 6000$, where $0{\cdot}4 < \Omega < 0{\cdot}5$ for unblown flows.

Different investigators have evaluated U_a^+ theoretically as different functions of V_w^+, depending upon whose experimental results they were attempting to fit. As pointed out by Black & Sarnecki (1958), one can develop numerous theories which describe U_a^+ and y_a^+ as functions of V_w^+, but the final test lies with the comparison with experimental data. Hence, in Simpson (1967), these relations were determined empirically from Simpson's data. Using the unblown constants $U_a^+ = y_a^+ = 11$ and $\Omega = 0{\cdot}44$, which seem to fit the low Reynolds number unblown data *as a whole*, U_a^+ was assumed to be independent of V_w^+ and the variation of y_a^+ was examined. Figures 5 to 7 show typical plots of ϕ *vs.* y^+ for several $\dot{m}''$ variations obtained by Simpson (1967), where

$$\phi = \frac{2}{V_w^+}[(1 + U^+ V_w^+)^{\frac{1}{2}} - (1 + 11\, V_w^+)^{\frac{1}{2}}],$$

for blown and sucked flows, and $\phi = U^+ - 11$ for unblown flows.

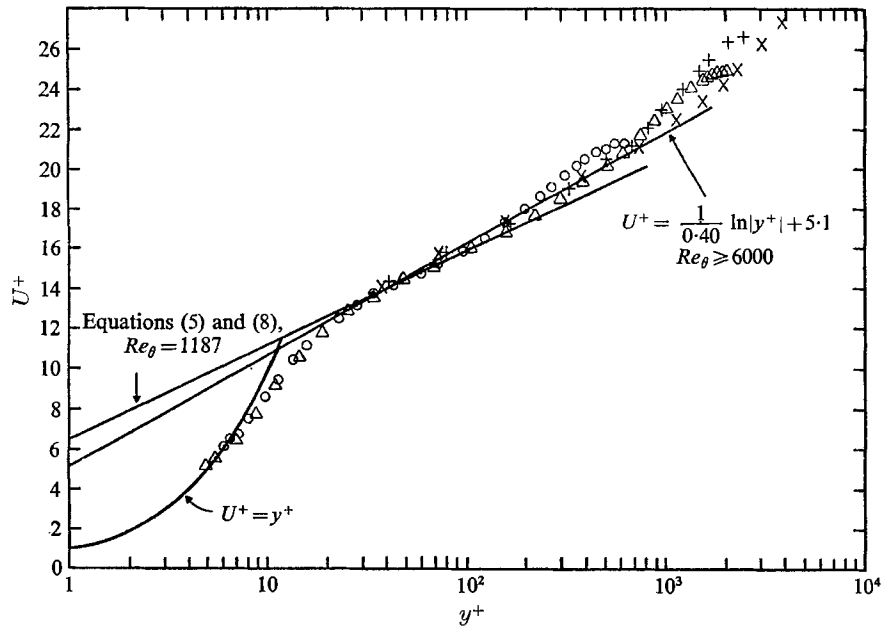

FIGURE 4. Unblown flat plate data.

	Simpson (1967)		Wieghardt (1943)	
	○	△	+	×
Re_θ	1187	4141	6144	15459
$\frac{1}{2}C_f \times 10^3$	2·20	1·65	1·42	1·21
y^+ at $\eta = 0{\cdot}1$	52	151	205	493

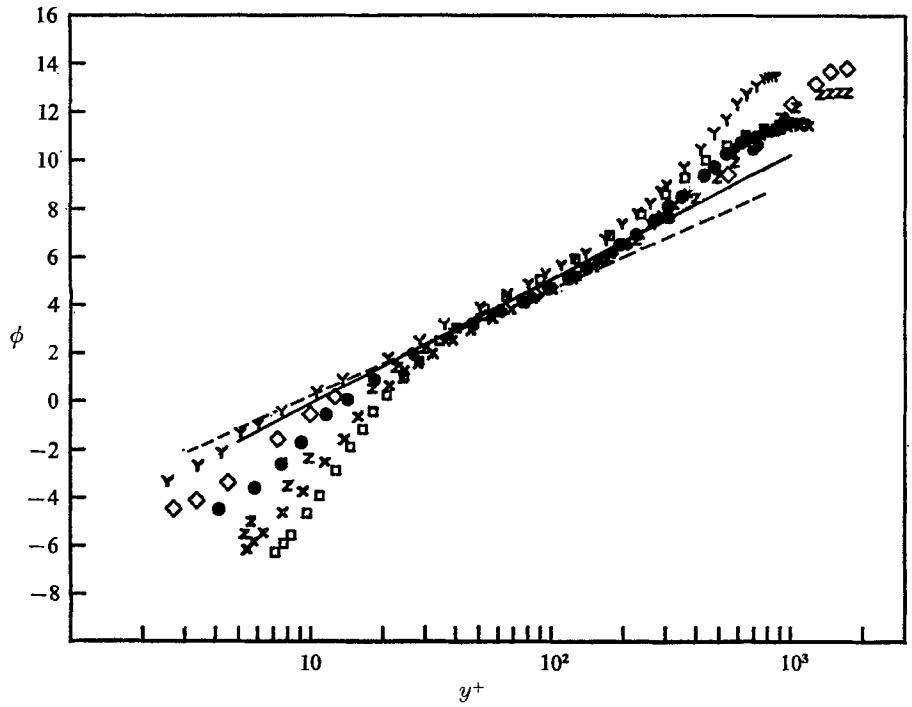

FIGURE 5. —, $\phi = 1/0{\cdot}44 \ln|y^+/11|$; - - -, equation (22), $Re_\theta = 10^3$: constant $\dot{m}''$ flows.

	□	×	z	Y	●	◇
$\dot{m}''/(\rho U)_\infty$	−0·0024	−0·0011	0·0000	0·0078	0·0019	0·0038
Re_θ	1015	1595	3177	9732	2480	9429

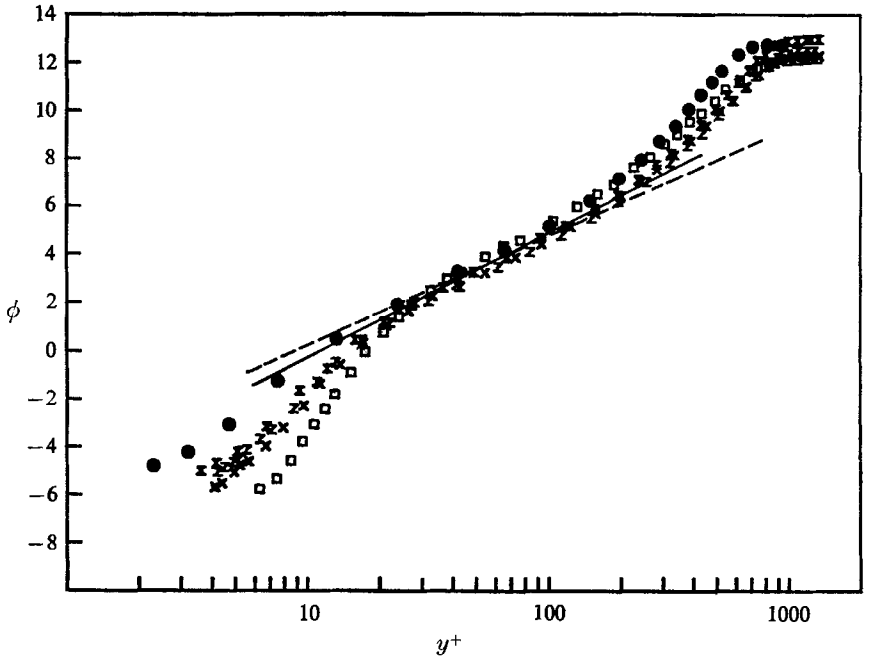

FIGURE 6. —, $\phi = 1/0{\cdot}44 \ln|y^+/11|$; - - -, equation (22), $Re_\theta = 10^3$: $\dot{m}'' \propto X^{-0{\cdot}2}$, constant B flows.

	□	×	z	⧖	●
B	−0·48	0·73	1·79	3·87	11·7
Re_θ	1557	2901	3673	4534	4813

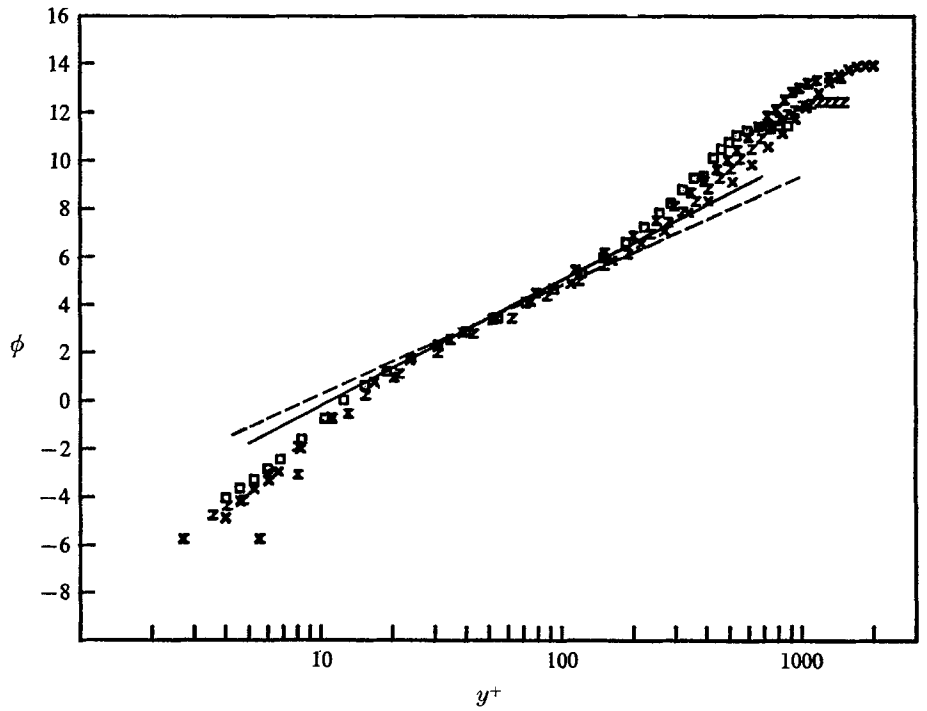

FIGURE 7. —, $\phi = 1/0{\cdot}44 \ln|y^+/11|$; - - -, equation (22), $Re_\theta = 10^3$:

	$\dot{m}'' \propto X^{-\frac{1}{2}}$ flow		$\dot{m}'' \propto X$ flow	
	□	×	z	⧖
$\dot{m}''/(\rho U)_\infty$	0·0046	0·0034	0·0034	0·0018
Re_θ	7172	4840	2695	6449

These data indicate that with $U_a^+ = 11$, the value y_a^+ in (15) is substantially independent of V_w^+. A definite logarithmic region exists for $30 < y^+ < 100$. Thus, (15) was written (Simpson 1967) in the form,

$$\frac{2}{V_w^+}[(1+U^+V_w^+)^{\frac{1}{2}}-(1+11V_w^+)^{\frac{1}{2}}] = \frac{1}{0{\cdot}44}\ln\left|\frac{y^+}{11}\right|. \tag{17}$$

Rather than go into great detail discussing the uncertainties in U^+, y^+ and ϕ associated with these data in the fully turbulent portion, several general remarks will be made. For $y^+ > 20$ the uncertainty in y^+ due to uncertainties in y are very small compared to uncertainties in U_τ. Likewise, for U^+ the main source of uncertainty is in U_τ, if we do not consider the failure to correct Pitot tube readings for turbulence as an error. Since $U_\tau = U_\infty(\frac{1}{2}C_f)^{\frac{1}{2}}$ for a constant property flow, the percentage uncertainty in U^+ and y^+ for a given traverse is approximately one half the percentage uncertainty given by Simpson *et al.* (1969) for $\frac{1}{2}C_f$.

The uncertainty in ϕ for a given traverse was found to be nearly equal to the numerical uncertainty in U^+, providing the uncertainty in U_a^+ is negligible. Figure 8 shows ϕ and its uncertainty envelope at $y^+ = 100$ for 63 traverses from flows with $\dot{m}'' =$ constant, $\dot{m}'' \propto x^{-0{\cdot}2}$, $\dot{m}'' \propto X$, and $\dot{m}'' \propto X^{-\frac{1}{2}}$. The average value of ϕ at $y^+ = 100$ for these traverses is 4·9, 2 % below the value given by (17). The uncertainty envelope may seem wide until one considers that a 5 % uncertainty in $\frac{1}{2}C_f$ for an unblown flow produces a 2·5 % uncertainty in determining $y^+ = 100$ and 8 % uncertainty in ϕ.

Based on five experimental profiles (Stevenson 1964) in the low Reynolds number range $1000 < Re_\theta < 6000$, Stevenson (1963*a*) proposed a fully turbulent portion mixing length relation,

$$\frac{2}{V_w^+}[(1+U^+V_w^+)^{\frac{1}{2}}-1] = \frac{1}{\Omega}\ln|y^+|+c, \tag{18}$$

where Ω and c are constants. Using 16 suction profiles and 8 blowing profiles from Mickley *et al.* (1954, 1957)†, Black & Sarnecki (1958) proposed

$$\frac{2}{V_w^+}[(1+U^+V_w^+)^{\frac{1}{2}}-(1+U_a^+V_w^+)^{\frac{1}{2}}] = \frac{1}{\Omega}\ln\left|\frac{y^+V_w^+}{\ln|1+U_a^+V_w^+|}\right|, \tag{19}$$

where U_a^+ are Ω are constants. This equation can be obtained from (15) and the second assumption of Rubesin (1954), i.e. U_a^+ is invariant with blowing, while y^+ is given by (11) with $U^+ = U_a^+$. Kendall (1959) also found that (19) fitted his experimental results, which are mainly for $Re_\theta < 6000$. With $\Omega = 0{\cdot}44$ and $U_a^+ = 11$, the values of ϕ at $y^+ = 100$ or ϕ_{100} are given by

$$\phi_{100} = \frac{1}{0{\cdot}44}\ln|100|+5{\cdot}55+\frac{2}{V_w^+}-\frac{2}{V_w^+}(1+11V_w^+)^{\frac{1}{2}}, \tag{20}$$

† The 1954 experimental results were criticized by Mickley & Davis (1957) as being unreliable. The 1957 $\frac{1}{2}C_f$ results have been recently shown by several investigators to have been obtained from the momentum integral equation without accounting for the small imposed pressure gradient. The corrected results of these investigators are presented by Simpson *et al.* (1969).

from (18), and

$$\phi_{100} = \frac{1}{0{\cdot}44} \ln \left| \frac{100 V_w^+}{\ln |1 + 11 V_w^+|} \right|, \tag{21}$$

from (19), and are shown on figure 8.

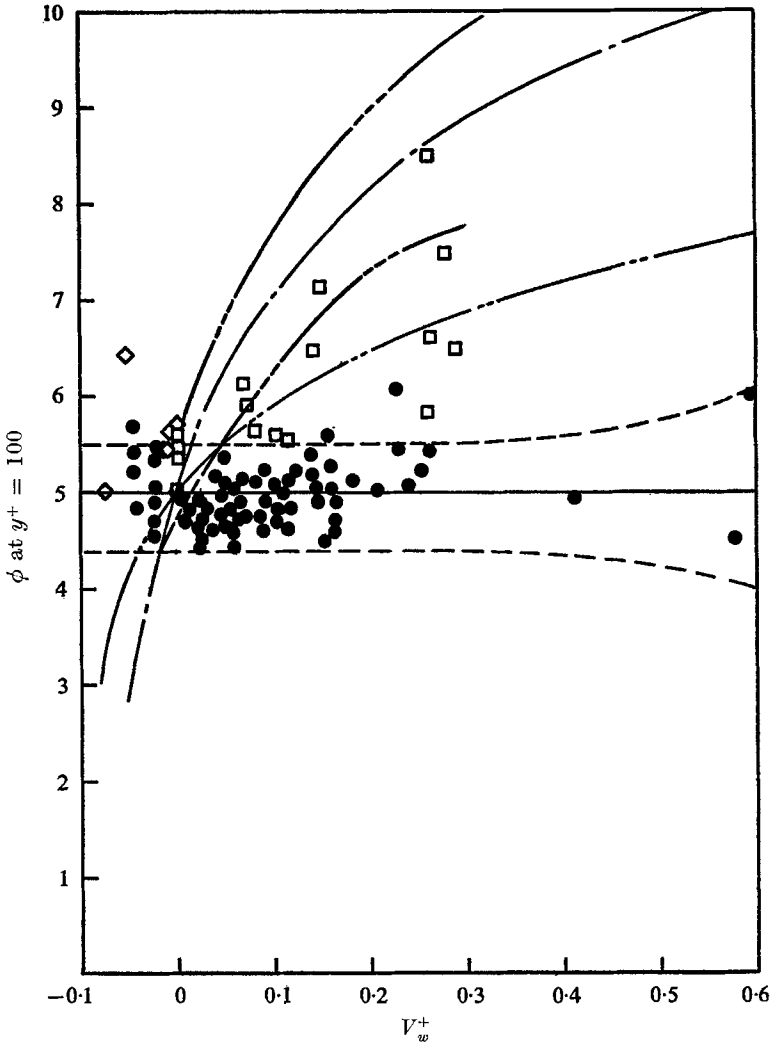

FIGURE 8. — · · · —, uncertainty envelope, Stevenson (1968); – –, uncertainty envelope, data of Simpson (1967); —, ϕ_{100} from (17), the 'law of the wall'; — · —, ϕ_{100} from (18), Stevenson's relation; — · · —, ϕ_{100} from (19), Black & Sarnecki's relation. □, data of Kendall (1959); ◇, of Favre *et al.* (1966); ●, of Simpson (1967).

Equation (17), evaluated at $y^+ = 100$, fits the present data better than (20) and (21). ϕ at any other y^+ in the fully turbulent portion, as given by (17), (18) and (19), differs by $1/0{\cdot}44 \ln |y^+/100|$ from ϕ_{100}. Thus the relatively large discrepancy between Stevenson's relation, (18), and Black & Sarnecki's relation, (19), and the experimental data of Simpson prevails throughout the fully

turbulent portion. Hence, (17) fits the fully turbulent data of Simpson much better than do Stevenson's relation (18) and Black & Sarnecki's relation (19).

The apparent discrepancy between (17), (18), and (19) is due primarily to differences in the experimental $\frac{1}{2}C_f$ values used by various investigators in determining these equations from experimental U^+ *vs.* y^+ and V_w^+ profiles.

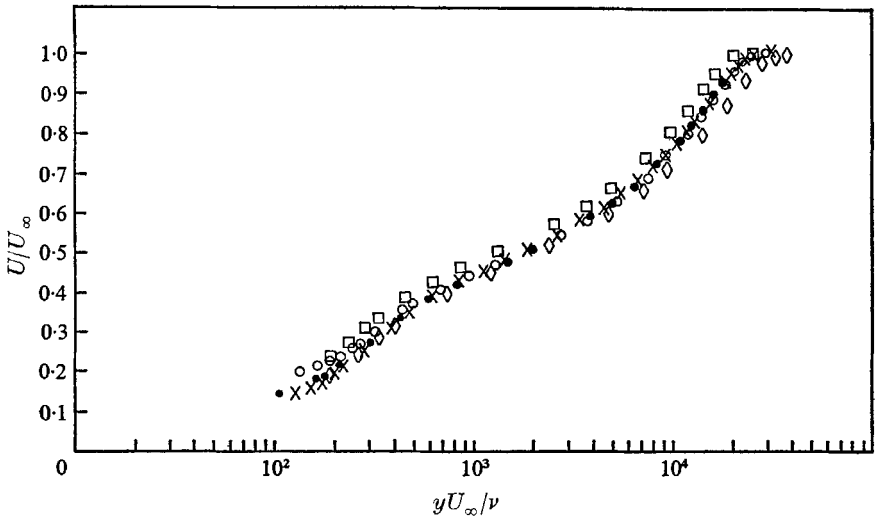

FIGURE 9. Data for given Re_θ and V_w/U_∞:

	Experimenter	Re_θ	V_w/U_∞	U_∞, ft./sec	$\frac{1}{2}C_f$
●	Simpson (1967)	3464	0·0034	41·94	0·00087
×		3484	0·00329	43·67	0·00093
○	McQuaid (1966)	3516	0·00327	51·06	0·00042
□	Kendall (1959)	2967	0·00321	50·1	0·00098
◇		4510	0·00327	50·2	0·00065

Figure 9 illustrates this point: data from Simpson (1967) and McQuaid (1966), for approximately the same Re_θ and V_w/U_∞, are found to be in good agreement in U/U_∞ *vs.* yU_∞/ν co-ordinates. There is reasonable agreement with Kendall's (1959) data, when one interpolates between his $Re_\theta = 2967$ and $Re_\theta = 4510$ profiles. However, McQuaid's $\frac{1}{2}C_f$ value is much lower than either Kendall's or Simpson's values, so this profile cannot correlate with the other profiles on a U^+*vs.* y^+ basis. Thus, the law of the wall supported by McQuaid's data must be different from the relations supported by the data of Kendall and Simpson.†

The data of Stevenson (1964) and McQuaid (1966) are shown by Stevenson (1968) to support (18) and lie with an uncertainty envelope for c when $\frac{1}{2}C_f$ is determined by the momentum integral equation and only $d\theta/dx$ is uncertain by $\pm$ 0·00015. (The momentum integral equation was the only independent means Stevenson (1964) and McQuaid (1966) used to obtain $\frac{1}{2}C_f$.) An uncertainty envelope for ϕ_{100} from (20) was calculated from Stevenson's uncertainty envelope for c and is shown on figure 8. Also shown on figure 8 are ϕ_{100} values obtained from

† Dr L. C. Squire of Cambridge University (1969) reports that (17) describes the data of McQuaid when the $\frac{1}{2}C_f$ results of Simpson (1967) at the same V_w/U_∞ and Re_θ are used in U_τ.

the data of Kendall (1959), which support (19) and (21). Because the data of Kendall fell below his uncertainty envelope for c, Stevenson (1968) concluded that the discrepancy between the experimental results of Stevenson and McQuaid and Kendall's results were possibly due to different surface roughness and porosity conditions.

In a comment on that work, Dahm & Kendall (1968) point out that $\frac{1}{2}C_f$ values from the two-dimensional momentum integral equation depend not only on the accuracy of $d\theta/dx$, but also on the accuracy of the blowing rate. They further illustrate that at a blowing rate V_w/U_∞ of 0·005 ($V_w^+ \approx 0{\cdot}26$) at $Re_x = 10^6$, $a \pm 1\,\%$ uncertainty in both $d\theta/dx$ and V_w/U_∞ yields about $\pm 32\,\%$ uncertainty in $\frac{1}{2}C_f$. They noted that Stevenson's data were obtained in a fully developed transpired region whose length is of the order of only 1 ft., making $d\theta/dx$ difficult to obtain accurately.

Kendall (1959) obtained $\frac{1}{2}C_f$ values by a sublayer technique similar to the one used by Simpson (1967) because of the difficulty of obtaining valid $\frac{1}{2}C_f$ values from the momentum integral equation at high blowing ($V_w/U_\infty > 0{\cdot}003$) on the apparatus. As pointed out in § 2, the momentum integral equation and sublayer $\frac{1}{2}C_f$ results of Simpson (1967) closely agree within experimental uncertainties estimated at 20:1 odds. Simpson *et al.* (1969) pointed out that Kendall's $\frac{1}{2}C_f$ results are in substantial agreement with Simpson's (1967) uniform injection results on a $(C_f/C_{f_0})_{Re_x}$ *vs.* b basis, Kendall's results being slightly lower at higher values of b. As shown on figure 8, ϕ_{100} from Kendall's data is best represented by Black & Sarnecki's relation, (19). However, with exception of the $V_w^+ \approx 0{\cdot}26$ data, ϕ_{100} from Kendall's data is nearly constant with V_w^+, which is not in gross disagreement with the form of (17).

All these $\frac{1}{2}C_f$ data have been obtained from velocity profile surveys in the flow. Direct $\frac{1}{2}C_f$ measurements with blowing using a floating balance are reported by Dershin, Leonard & Gallaher (1967) for a 3·18 Mach number flat plate flow. These results agreed closely with Rubesin's (1954) theory, which was found to agree closely with the subsonic $\frac{1}{2}C_f$ results of Simpson and of Kendall on a $(C_f/C_{f_0})_{Re_x}$ *vs.* b basis (Simpson *et al.* 1969). Hence although some discrepancy between the various $\frac{1}{2}C_f$ results may be due to different surface roughness and porosity conditions, results from the momentum integral equation are very sensitive to small errors in $d\theta/dx$ and V_w/U_∞, which possibly accounts for some of the gross discrepancy between the U^+ *vs.* y^+ and V_w^+ results of Stevenson and McQuaid, and the results of Kendall and Simpson. Thus, if we believe the $\frac{1}{2}C_f$ results of Simpson, (17) is a plausible 'law of the wall with blowing' using a constant Ω for the range $1000 < Re_\theta < 6000$.

Unlike the injection case, the transpiration term for suction is added to the momentum thickness gradient to obtain $\frac{1}{2}C_f$ from the two-dimensional momentum integral equation, yielding very accurate results. Note that the terms in $(1 + U^+V_w^+)^{\frac{1}{2}}$ and $(1 + 11V_w^+)^{\frac{1}{2}}$ tend to cancel, making ϕ sensitive to small errors in velocity. Thus, the experimental difficulties with obtaining suction data lie with making and using very small probes for accurate velocity surveys of the thin boundary layers.†

† For footnote see facing page.

All suction results shown in figure 8 are for undersucked layers, $d\theta/dx > 0$, that possess the 'wake component' or departure from a logarithmic inner region equation in the outer region. No turbulent critical layers, $d\theta/dX = 0$, were reported by Simpson (1967) although three oversucked layers, $d\theta/dx < 0$, that possessed laminar asympototic velocity profiles were recorded. One $\dot{m}'' \propto X^{-0.2}$ layer with $d\theta/dx > 0$ appeared to have no wake component until near the exit of the flow channel, indicating a strong influence of the high suction near the channel entrance. It is interesting to note that V_w/U_∞ at the channel entrance for this flow was about the same as for one of the uniform suction flows with $d\theta/dx < 0$. Also shown in figure 8 are ϕ_{100} results from the data of Favre *et al.* (1966) for undersucked layers. Both sets of data support (17) as a 'law of the wall for undersucked layers', using a constant Ω for the range $1000 < Re_\theta < 6000$.

As discussed in § 5, the Reynolds number variation of Ω in the range $1000 < Re_\theta < 6000$ with blowing and suction is the same as for the unblown case. If we incorporate this variation of Ω while not disturbing the blowing and suction correlation of (17), it is sufficient to write

$$\phi = \frac{1}{\Omega} \ln \left| \frac{y^+}{11} \right| + M(Re_\theta), \tag{22}$$

where $\Omega = 0{\cdot}40\ (Re_\theta/6000)^{-\frac{1}{8}}$, and

$$M(Re_\theta) = Re_\theta^{\frac{1}{8}}[9{\cdot}92 - 0{\cdot}732 \ln |Re_\theta|] - 11,$$

for $Re_\theta < 6000$ and $\Omega = \kappa = 0{\cdot}40$ and $M(Re_\theta) = 0{\cdot}10$ for $Re_\theta > 6000$. Equation (22) reduces to (5) and (8) for zero blowing, and (17) when $\Omega = 0{\cdot}44$. As for the unblown case, the logarithmic relation (22) pivots (figures 5–7) within the logarithmic region for $1000 < Re_\theta < 6000$ and near universal ϕ *vs.* y^+ similarity is obtained. Note that, as in the unblown case, the Re_θ variation of Ω cannot be strongly detected by ϕ *vs.* y^+ data but requires examination of the 'velocity defect' data representation and the existence of a logarithmic overlap region.

4.2 *The velocity defect law*

Stevenson (1963*b*) proposed an extension of (2) and (4), the unblown velocity defect relation, to the outer region of blown and undersucked boundary layers. This relation is

$$\Gamma = \frac{2}{V_w^+}[(1+B)^{\frac{1}{2}} - (1 + U^+ V_w^+)^{\frac{1}{2}}] = F(\Pi, \eta), \tag{23}$$

which reduces to (2) when $V_w = 0$. He also presented a more general dimensional similarity argument for a logarithmic overlap region than that presented by Millikan. He found that the sufficient condition for a logarithmic overlap region between the inner flow, represented by (15), and the outer flow, described by

† Simpson (1967) noted that without making stagnation pressure gradient and wall effects corrections, experimental laminar asymptotic suction profiles could be obtained within a few ten-thousandths of an inch of the theoretical curves with his probes. This discrepancy was smaller than the estimated uncertainty of locating a probe with respect to the test wall.

(23), is that the form of the term containing U is the same for each region, i.e. $2(1+U^+V_w^+)^{\frac{1}{2}}/V_w^+$.

As in the unblown case, the data for flows with constant V_w (figure 10) and $V_w \propto X^{-0.2}$ (figure 11) show a definite U/U_∞ *vs.* η similarity independent of Re_θ in

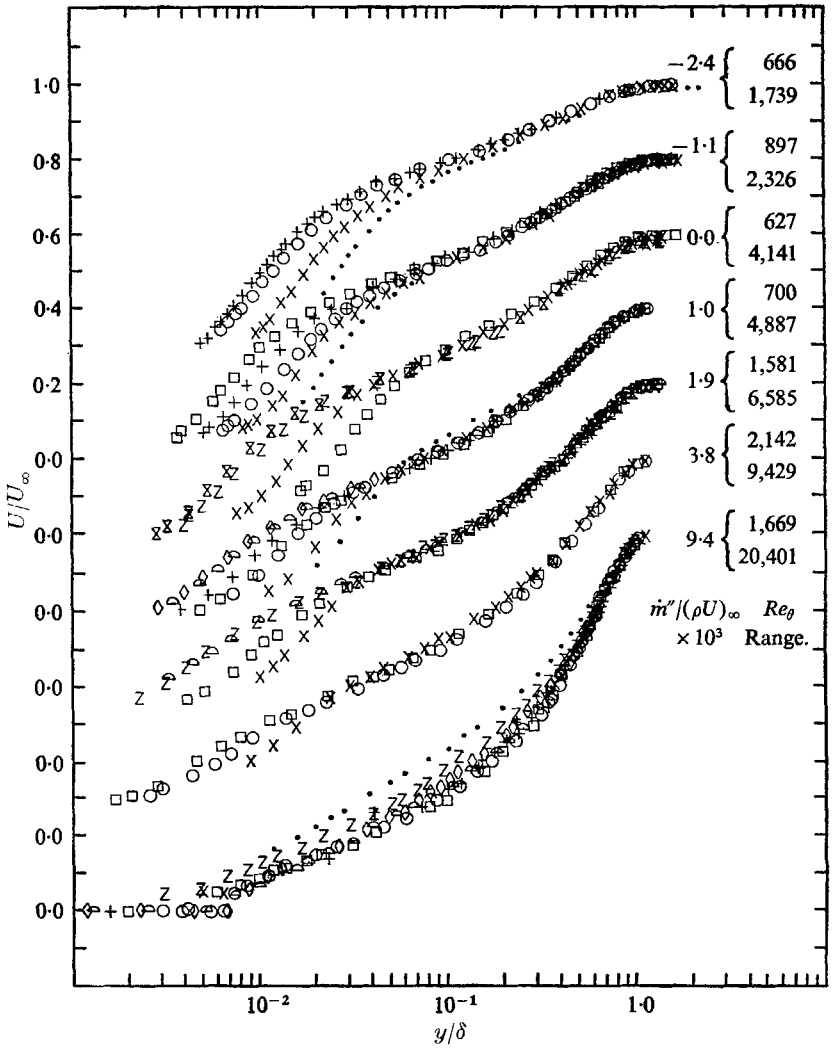

FIGURE 10. U/U_∞ *vs.* y/δ from constant $\dot{m}''$ flows.

the region outside the sublayer for $1000 < Re_\theta < 6000$. As shown in figures 10 and 11, there is a detectable departure from this outer region similarity at higher Reynolds number. As a logical extension of the low Reynolds number velocity defect relation, (6), it is proposed that

$$\Gamma = \frac{2}{V_w^+}[(1+B)^{\frac{1}{2}} - (1+U^+V_w^+)^{\frac{1}{2}}] = E(\eta, \Pi, Re_\theta), \tag{24}$$

where

$$E(\eta, \Pi, Re_\theta) = \frac{1}{\Omega(Re_\theta)}[-\ln|\eta| + \Pi(2-\omega(\eta))],$$

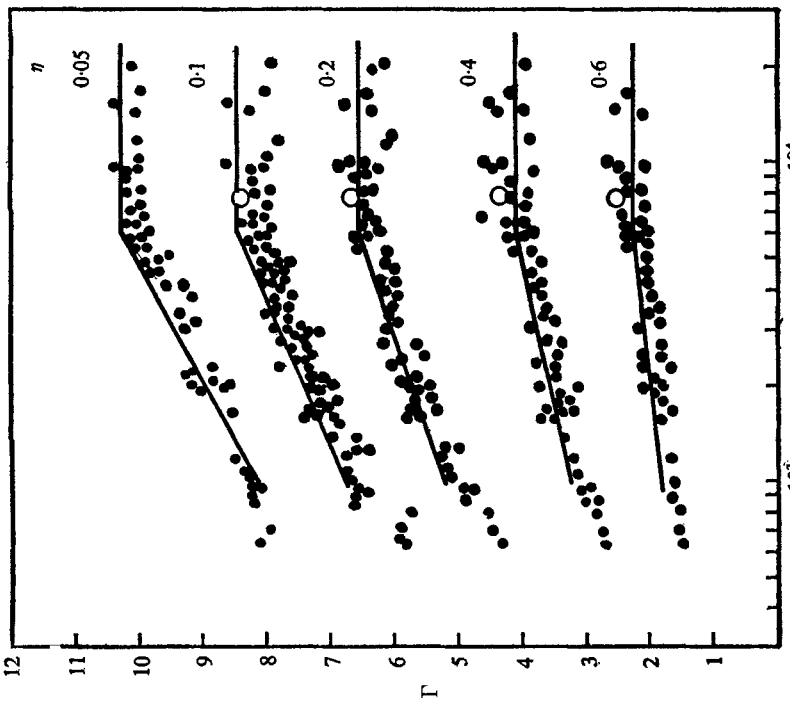

FIGURE 12. Injection and suction velocity defect law (constant η). ●, data of Simpson (1967), blowing and suction; ○, of Klebanoff (1954), no blowing. —, equation (24), $\Omega = 0{\cdot}40\ (Re_\theta/6000)^{-\frac{1}{8}}$, $1000 < Re_\theta \leqslant 6000$, and $\Omega = 0{\cdot}40$ $Re_\theta > 6000$.

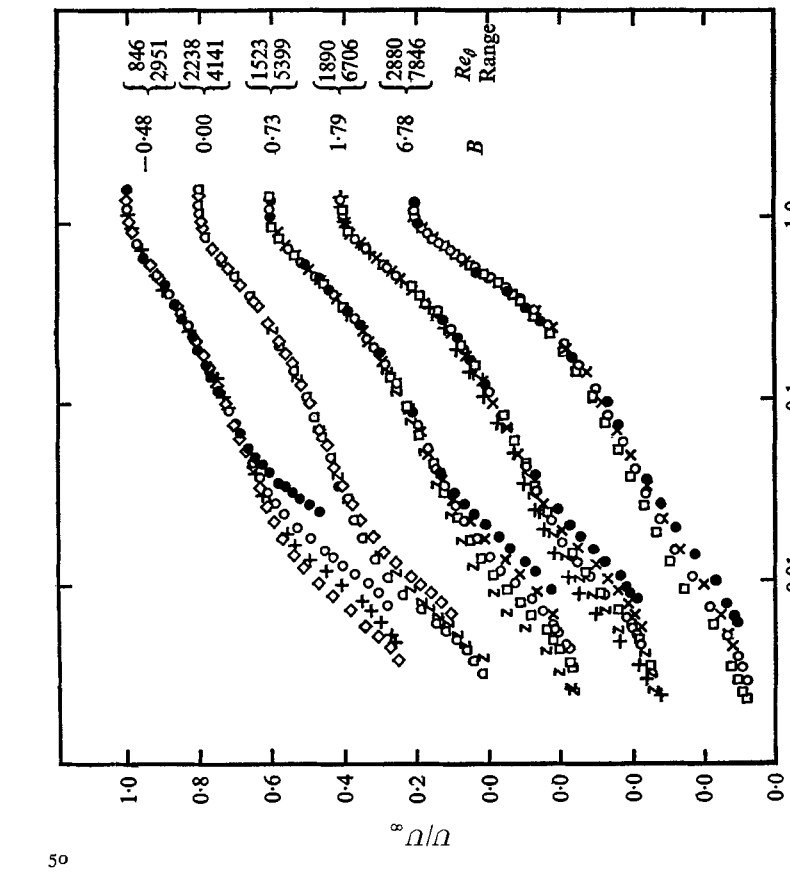

FIGURE 11. U/U_∞ *vs.* y/δ from constant B flows.

and $\Omega = 0{\cdot}40\ (Re_\theta/6000)^{\frac{1}{8}}$, for $Re_\theta < 6000$, and $\Omega = \kappa = 0{\cdot}40$, for $Re_\theta > 6000$. As shown in figure 12, this hypothesis fits the experimental results of Simpson (1967) for 94 profiles from flows with no blowing, constant V_w, $V_w \propto X^{-0{\cdot}2}$, $V_w \propto X$ and $V_w \propto X^{-\frac{1}{2}}$.†

5. Eddy viscosity and mixing length distributions for transpired flows

Presently, there are many turbulent boundary-layer prediction methods (Kline *et al.* 1968). Several of these methods relate the mean turbulent shear stress in the momentum boundary-layer equation to the velocity profile by mixing length theory,

$$\tau_t \equiv \rho l^2 \frac{\partial U}{\partial y}\left|\frac{\partial U}{\partial y}\right|, \tag{25}$$

and a model equation for l, or by Boussinesq's 'eddy' viscosity theory,

$$\frac{\tau_t}{\rho} \equiv \epsilon_m \frac{\partial U}{\partial y}, \tag{26}$$

with a relation for ϵ_m, where subscript t denotes turbulent contribution. To extend these methods to cases with blowing and suction, shear stress variations through the boundary layer must be determined to extract l and ϵ_m from mean velocity profile data.

5.1. *Shear stress profiles*

Shear stress profiles were computed for the fully turbulent flows with $\dot{m}'' =$ constant and $\dot{m}'' \propto X^{-0{\cdot}2}$. These profiles were based on the momentum and continuity equations and experimental velocity profiles.

5.1.1. *Boundary layer equations.* Consider the two-dimensional X-momentum and continuity boundary-layer equations for uniform free-stream velocity,

$$\frac{\partial}{\partial X}\left(\frac{\rho U^2}{\rho_\infty U_\infty^2}\right)+\frac{\partial}{\partial y}\left(\frac{\rho U V}{\rho_\infty U_\infty^2}\right) = \frac{\partial(\tau/\rho_\infty U_\infty^2)}{\partial y} \quad \text{(momentum)}, \tag{27}$$

$$\frac{\partial}{\partial X}\left(\frac{\rho U}{\rho_\infty U_\infty}\right)+\frac{\partial}{\partial y}\left(\frac{\rho V}{\rho_\infty U_\infty}\right) = 0 \quad \text{(continuity)}. \tag{28}$$

Rearranging (27) and (28), integrating each equation with respect to y, and applying the conditions $\rho V/\rho_\infty U_\infty = \rho_w V_w/\rho_\infty U_\infty$ and $\tau = \tau_w$ at $y = 0$ yields

$$\frac{\partial}{\partial X}\int_0^y \frac{\rho U^2}{\rho_\infty U_\infty^2}\,dy+\frac{\rho_w V_w U}{\rho_\infty U_\infty^2}\bigg|_y-\frac{U}{U_\infty}\frac{\partial}{\partial X}\int_0^y \frac{\rho U}{\rho_\infty U_\infty}\,dy = \frac{\tau-\tau_w}{\rho_\infty U_\infty^2}, \tag{29}$$

† Mickley *et al.* (1963, 1964, 1965) modified the constant Ω unblown defect relation, (4), for blown flows by substituting τ_{max}, the maximum shear stress in a blown boundary layer, for τ_w in U_τ. However, this conclusion was partly based on results obtained from using the uncorrected Mickley–Davis $\frac{1}{2}C_f$ values. The results of Smith (1962) and Fraser (1964) were also used to support this conclusion, although acceptable $\frac{1}{2}C_f$ values for the unblown case were reported by neither author. (Fraser fitted (4) to his unblown profiles, $Re_\theta < 6000$, and obtained a nearly constant $\frac{1}{2}C_f$ value. Had he used (6), he would have obtained the $\frac{1}{2}C_f \sim Re_\theta^{-\frac{1}{8}}$ variation.) The data of Simpson (1967) fail to support the Mickley *et al.* hypothesis.

when the resulting continuity equation is substituted into the momentum equation.

5.1.2. *Shear stress profile computing equations.* The numerical differentiation of experimental boundary-layer data with respect to X produces uncertain results when only a few X-stations are available. Therefore, the following assumptions were employed to evaluate the left side of (29);

(i) U/U_∞ *vs.* y/δ similarity in the outer region, i.e. X dependency contained in δ.

(ii) The contribution of the convective terms in the momentum equation is very small in the inner region where assumption (i) fails.

(iii) $\dfrac{1}{\theta}\dfrac{d\theta}{dx} \simeq \dfrac{1}{\delta}\dfrac{d\delta}{dx}$.

Using those assumptions in (29), and integrating by parts, yields the shear stress profile computing equation,

$$\frac{\tau-\tau_w}{\rho_\infty U_\infty^2} = \frac{1}{\theta}\frac{d\theta}{dx}\left(\int_0^y \frac{\rho U^2}{\rho_\infty U_\infty^2}\,dy - \frac{U}{U_\infty}\int_0^y \frac{\rho U}{\rho_\infty U_\infty}\,dy\right) + \frac{\rho_w V_w U}{\rho_\infty U_\infty^2},$$

(combined momentum and continuity) (30)

for flows with negligible ρ/ρ_∞ variations through the boundary layer. Equation (30) reduces to the two-dimensional momentum integral equation when $y\to\infty$:

$$\frac{\tau_w}{\rho_\infty U_\infty^2} = \tfrac{1}{2}C_f = \frac{d\theta}{dX} - \frac{\rho_w V_w}{\rho_\infty U_\infty}. \tag{31}$$

5.1.3. *Discussion of the shear stress results.* Consider the validity of the above assumptions. Assumption (i) has been shown in §4.2 to be valid in the outer 90 % of a layer for all fully turbulent flows with $\dot{m}''$ = constant and $\dot{m}''\propto X^{-0\cdot2}$. Because this assumption is not valid for the flows with $\dot{m}''\propto X$ and the $\dot{m}''\propto X^{-\frac{1}{2}}$, no shear stress profiles were generated for these cases.

Assumption (ii) is concerned with the contribution from the inner region, where assumption (i) fails, to the convective quantity,

$$\theta_r = \int_0^y \frac{\rho U^2}{\rho_\infty U_\infty^2}\,dy - \frac{U}{U_\infty}\int_0^y \frac{\rho U}{\rho_\infty U_\infty}\,dy, \tag{32}$$

contained in (30). The terms on the right side of (32) tend to cancel, and are small near the wall. A survey of 30 profiles showed that $(\theta_r/\theta)\,(d\theta/dX)$ contributed less than 2 % to the right side of (30),

$$\frac{\tau-\tau_w}{\rho U_\infty^2} = \frac{\theta_r}{\theta}\frac{d\theta}{dX} + \frac{\rho_w V_w U}{\rho_\infty U_\infty^2}, \tag{33}$$

at the inner edge of the U/U_∞ *vs.* y/δ similarity region.

Assumption (iii) is useful for several reasons. It allows (30) to reduce to the two-dimensional momentum integral equation (31) as $y\to\infty$. Secondly, it allows $d\theta/dX$ to be replaced by $\frac{1}{2}C_f + (\rho_w V_w/\rho_\infty U_\infty)$ to ensure that $\tau/\rho_\infty U_\infty^2 \to 0$ as $y\to\infty$. For all profiles used to generate $\tau/\rho_\infty U_\infty^2$, (iii) was found to hold within 5 %, using $\frac{1}{2}C_f$ and $\rho_w V_w/\rho_\infty U_\infty$ to obtain $d\theta/dX$ and finite differences to obtain $d\delta/dX$.

Simpson (1967) presented all τ/τ_w profiles generated for the present turbulent flows with $\dot{m}'' =$ constant and $\dot{m}'' \propto X^{-0.2}$. To be valid these profiles must satisfy the integral momentum and continuity equations. Since the two-dimensional momentum integral equation is built into (30), it is satisfied by the shear profiles.

The shear profiles should certainly satisfy the so-called 'mechanical energy equation'

$$U\frac{\partial(\rho U^2)}{\partial X}+U\frac{\partial(\rho UV)}{\partial y}=U\frac{\partial \tau}{\partial y}, \tag{34}$$

which is nothing more than (27) multiplied by U. Using (28), integrating with respect y, and letting $y\to\infty$, results in the 'integral mechanical energy equation',

$$\frac{1}{2}\left[\frac{d\theta^*}{dX}-\frac{\rho_w V_w}{\rho_\infty U_\infty}\right]=\int_0^1 \frac{\tau}{\rho_\infty U_\infty^2}\,d\left(\frac{U}{U_\infty}\right), \tag{35}$$

with

$$\theta^*=\int_0^\infty \frac{\rho U}{\rho_\infty U_\infty}\left(1-\frac{U^2}{U_\infty^2}\right)dy$$

for constant free-stream velocity blown flows. For unblown flows, (35) reduces to the form presented by Rotta (1962). The $d\theta^*/2dX$ term of (35) has been interpreted by Rotta as the rate of loss of mechanical energy in the boundary layer. The $\rho_w V_w/2\rho_\infty U_\infty$ term represents the rate at which mechanical energy is absorbed by the blown fluid. The

$$\int_0^1 \left(\frac{\tau}{\rho_\infty U_\infty^2}\right)d\left(\frac{U}{U_\infty}\right)$$

term represents the rate of dissipation of mechanical energy produced by the mean shear stresses.

The left side of (35) can be obtained directly from data, independent of any assumptions used to generate shear profiles. The right side can be deduced from the generated shear stress profiles. For each run, a power fit of the form hRe_x^p was made of

$$Re_{\theta^*}-\int_0^{Re_x}\frac{\rho_w V_w}{\rho_\infty U_\infty}\,d(Re_x).$$

Differentiating the result produces $hp\,Re_x^{p-1}$ for the left side of (35). The right side is easily fitted by kRe_x^q. For flows with $\dot{m}'' =$ constant the right side is found to be no more than 4 % different from the left side at $Re_x = 10^6$, as shown by Simpson (1967). In the cases $\dot{m}'' \propto X^{-0.2}$ there is at most a 3·5 % difference. As shown by Simpson (1967), the difference is in most cases less than 1 %. It is concluded that the shear profiles satisfy the integral momentum, continuity, and 'mechanical energy' equations to a good degree.

Typical shear stress profiles for blown flows are normalized on the *maximum* shear stress and presented in figures 13 and 14 against U/U_∞ for the cases $\dot{m}'' =$ constant and $\dot{m}'' \propto X^{-0.2}$. As one can see, near the wall the profiles are nearly linear and can be described by

$$\tau=\tau_w+\rho_w UV_w, \tag{36}$$

which is equivalent to (30) when convective terms are neglected. A maximum value is seen to occur near $U/U_\infty = 0{\cdot}63$. (Wooldridge & Muzzy 1966 also report

the maximum shear stress at $U/U_\infty \simeq 0{\cdot}6$ for $0 < B < 20$.) This maximum existed for all blown shear stress profiles. In the outer portion ($U/U_\infty > 0{\cdot}635$), all blown $\tau/\tau_{\max}$ *vs.* U/U_∞ profiles lie on a single curve independent of $\dot{m}''$.

All these profiles have been generated for $Re_\theta < 15{,}000$ with the majority in

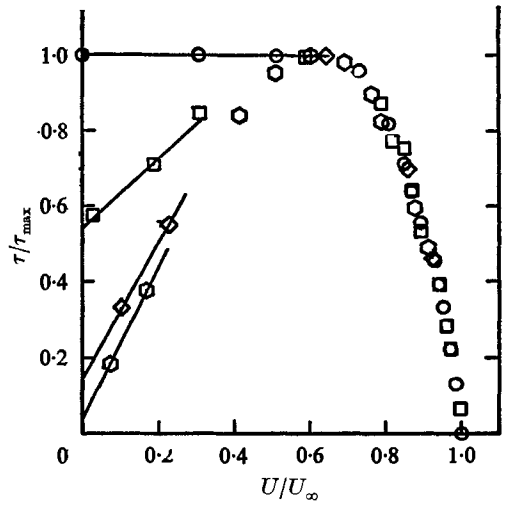

FIGURE 13. —, $\tau/\tau_{\max} = \tau_w/\tau_{\max} + \rho_w V_w U/\tau_{\max}$: constant $\dot{m}''$ flows.

	○	□	◇	⬡
$\dot{m}''/(\rho U)_\infty$	0·000	0·0019	0·0038	0·0095
Re_θ	3177	5093	7130	14940

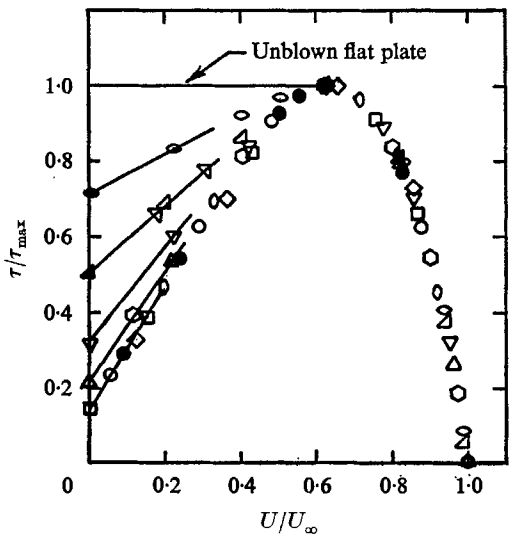

FIGURE 14. —, $\tau/\tau_{\max} = \tau_w/\tau_{\max}[1 + BU/U_\infty]$: constant B flows.

	●	0	○	□	◇	⬡	△	▽	◹	◿	○
B	11·7	11·7	11·7	11·7	11·7	6·78	6·78	3·88	1·79	1·79	0·78
Re_θ	3253	4813	6366	9181	11661	2880	4145	3464	2706	3673	2901

the range $Re_\theta < 6000$, where the constant $\Omega, \kappa = 0{\cdot}40$, blown and sucked velocity defect law does not hold. Hence, these results for the outer portion and the apparent point of maximum shear should not be extrapolated for $Re \gg 6000$.

5.2. *Eddy viscosity and mixing length experimental results*

The quantities ϵ_M and l/δ follow from the generated shear stress profile, (25) and (26), and the gradient $\partial U/\partial y$. Since the numerical differentiation of experimental data can be difficult and the resulting values questionable, the following procedure was used in obtaining $\partial U/\partial y$.

Polynomial least squares curve fits of the form,

$$\kappa_{ij}(y) = \sum_{n=0}^{n=i} a_n Z(y)^n, \tag{37}$$

and of degree i were made for a given U/U_∞ *vs.* y data profile at a given X station for the j number of nearest data points surrounding and including a given point of interest. The first derivative of (37), for a given point, produced the derivative $\partial(U/U_\infty)/\partial y$ for that point. The ϵ_M/ν and l/δ results from four different fits of the same velocity profile were examined to determine the degree of bias in ϵ_M/ν and l/δ produced by the choice of polynomial fit. The polynomial fits tested contained: (i) $i = 1$, $j = 5$, and $Z(y) = y$; (ii) $i = 3$, $j = 5$, and $Z(y) = y$; (iii) $i = 2$, $j = 7$, and $Z(y) = y$; and (iv) $i = 2$, $j = 5$, and $Z(y) = \ln|y|$. For a given velocity profile, the resulting ϵ_M/ν and l/δ profiles differed, respectively, by no more than 5 % depending on the choice of polynomial fit. The results for $i = 2$, $j = 5$, and $Z(y) = y$ are presented here.

It is well known (Rotta 1962; Hinze 1959) that, near the wall, the flow is governed by the wall condition, molecular viscosity, and small-scale turbulence. In the outer region of an unblown layer, eddy motion determines the momentum transport with the mean velocity profile, dimensionless eddy viscosity $\epsilon_M/\nu^* U_\infty$ and mixing length l/δ profiles correlating on η (Rotta 1962; Escudier 1965) and slightly on Re_θ, as will be discussed below. Thus, ν plays a rather small role in this region, being contained explicitly only in Re_θ.

The present values for the unblown ϵ_M/ν profiles near the wall are shown in figure 15 with ϵ_M/ν results from hot-wire anemometer data using the results of Kline (1965) from the data of Klebanoff (1954) and the results of Hinze (1959) from the data of Schubauer (1954). For a given y^+ the present results agreed within 5 % and within the scatter of the Kline and Hinze results for the region of U^+ *vs.* y^+ similarity and $y^+ > 20$ ($\epsilon_M/\nu > 4$). This good agreement with previously obtained eddy viscosity results supports the general acceptability of the present method in obtaining ϵ_M/ν and l/δ.

5.2.1. *The wall region.* In figure 16, ϵ_M/ν near the wall is shown as a strong function of V_w^+ as well as y^+, although correlation parameters are not obvious.†

† As added evidence of the surface smoothness, it was assumed (Simpson 1967), as in the unblown case, that the surface is aerodynamically smooth with transpiration if the r.m.s. roughness height κ_w remains in the viscous sublayer. Using the sublayer thickness as half the y^+ where $\epsilon_M/\nu = 1$, yields $\kappa_w U_\tau/\nu \ll y^+$ of the sublayer.

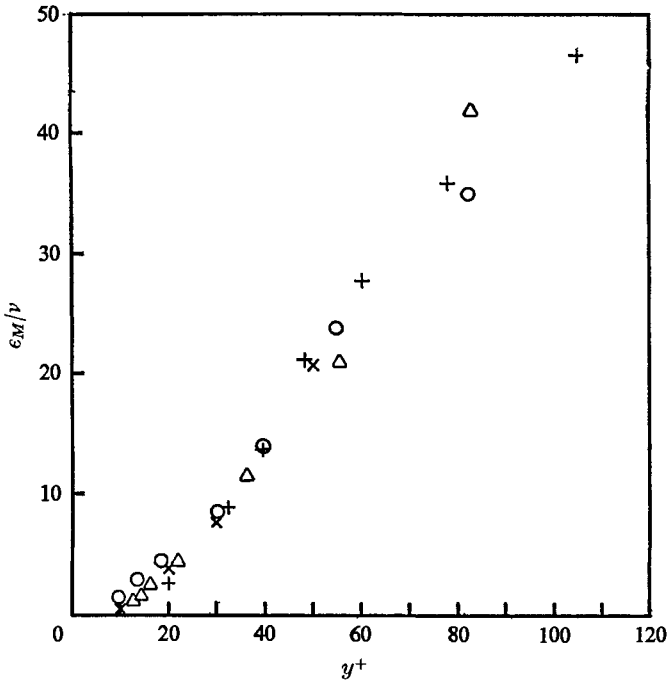

FIGURE 15. $V_w/U_\infty = 0$. △, Kline's (1965) result from Klebanoff's (1954) data; ×, Hinze's (1959) result from Schubauer's (1954) data. Simpson's (1967) data: □, $Re_\theta = 2238$; ○, 3177; +, 4318.

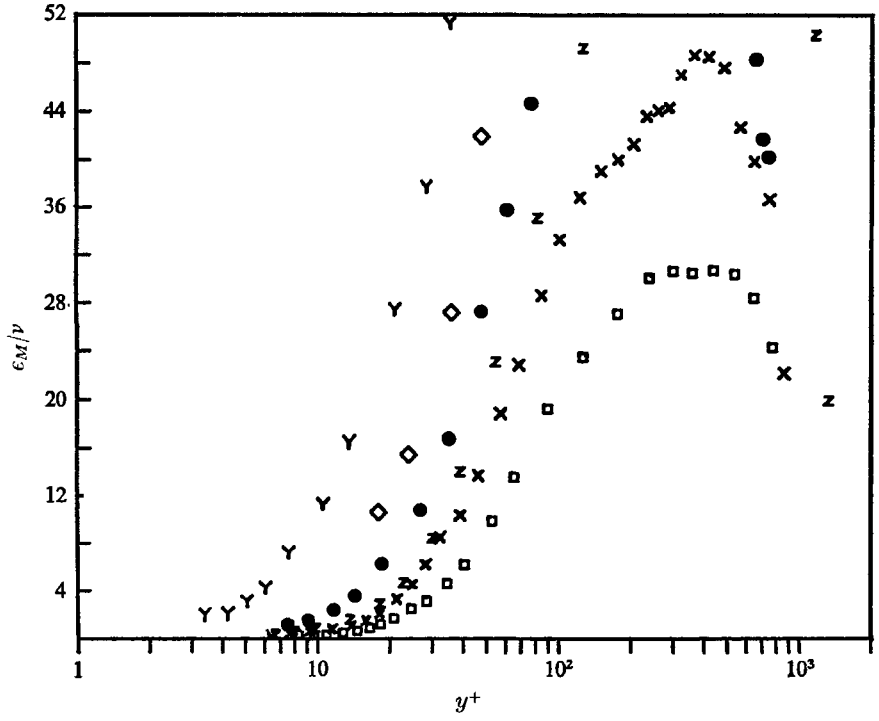

FIGURE 16. ϵ_M/ν *vs.* y^+ for given V_w^+: constant $\dot{m}''$ flows.

	□	×	Z	Y	●	◇
V_w^+	−0·0434	−0·0219	0	0·5826	0·0512	0·1606
Re_θ	1015	895	3177	9722	2480	9429

In order to develop correlation parameters relating ϵ_M/ν, V_w^+ and y^+ (or U^+), the ideas of Spalding (1961) and Kleinstein (1967) will be used:

(i) $\epsilon_M/\nu \sim y^{+3} \sim U^{+3}$ in the viscous sublayer, according to the work of Reichardt (Rotta 1962).

(ii) ϵ_M/ν must be consistent with the velocity profile correlation of the logarithmic region.

Thus, using (13) and (26) we obtain

$$(1 + U^+ V_w^+) = \left(1 + \frac{\epsilon_M}{\nu}\right) \frac{dU^+}{dy^+}. \tag{38}$$

Equations (14) and (26) can be combined to obtain

$$\frac{\epsilon_M}{\nu} = \Omega^2 y^{+2} \frac{dU^+}{dy^+} \tag{39}$$

for the logarithmic part of the wall region. Combining (38) and (39), we obtain

$$\left(1 + \frac{\epsilon_M}{\nu}\right) \frac{\epsilon_M}{\nu} = \Omega^2 y^{+2} (1 + U^+ V_w^+),$$

which becomes

$$\frac{\epsilon_M}{\nu} = \Omega y^+ (1 + U^+ V_w^+)^{\frac{1}{2}} \tag{40}$$

for the logarithmic region when $\epsilon_M/\nu \gg 1$. Using (22) to describe y^+ as a function of U^+, V_w^+, and Re_θ produces

$$\epsilon_M/\nu = 11\psi(1 + U^+ V_w^+)^{\frac{1}{2}} \exp\{\psi - \psi_a - M(Re_\theta)\} \tag{41}$$

where

$$\psi = \frac{2\Omega}{V_w^+} [(1 + U^+ V_w^+)^{\frac{1}{2}} - 1],$$

and

$$\psi_a = \frac{2\Omega}{V_w^+} [(1 + 11 V_w^+)^{\frac{1}{2}} - 1].$$

It is necessary to subtract the first three terms of $\exp\{\psi\}$ from $\exp(\psi)$ in order to satisfy the Reichardt condition in the viscous sublayer. (Since $\exp\{\psi\}$ is much larger than the subtracted polynomial terms, little effect of this subtraction is seen in the logarithmic region.) Thus, rearranging (41) we obtain

$$\frac{(\epsilon_M/\nu) \exp\{\psi_a + M(Re_\theta)\}}{11\psi(1 + U^+ V_w^+)^{\frac{1}{2}}} = Q = \exp\{\psi\} - (1 + \psi + \tfrac{1}{2}\psi^2). \tag{42}$$

The generated ϵ_M/ν results are shown in figures 17–19 in the form of Q *vs.* ψ. In the wall region there is a correlation of the blowing results within 20 % using these parameters. This correlation is fair considering that the uncertainty associated with ϵ_M/ν is about ± 10 %. The outer region results of course do not correlate on these wall region parameters. The scatter in the innermost region of each profile is due to the uncertainties of the present method in obtaining ϵ_M/ν from $(1 + [\epsilon_M/\nu])$ as $\epsilon_M/\nu < 1$ in the sublayer. The unblown and suction profiles are in poorest correlation with the blown profiles, being about 50 % lower for $\psi \simeq 5$.

Equation (42) is shown in figures 17–19 to be within 20 % agreement with the blown results in the wall region. The unblown and suction results do not closely agree with (42), being about 50 % lower. Thus, while ϵ_M/ν varies strongly with V_w^+ and y^+, it can be substantially correlated with the variables Q and ψ.

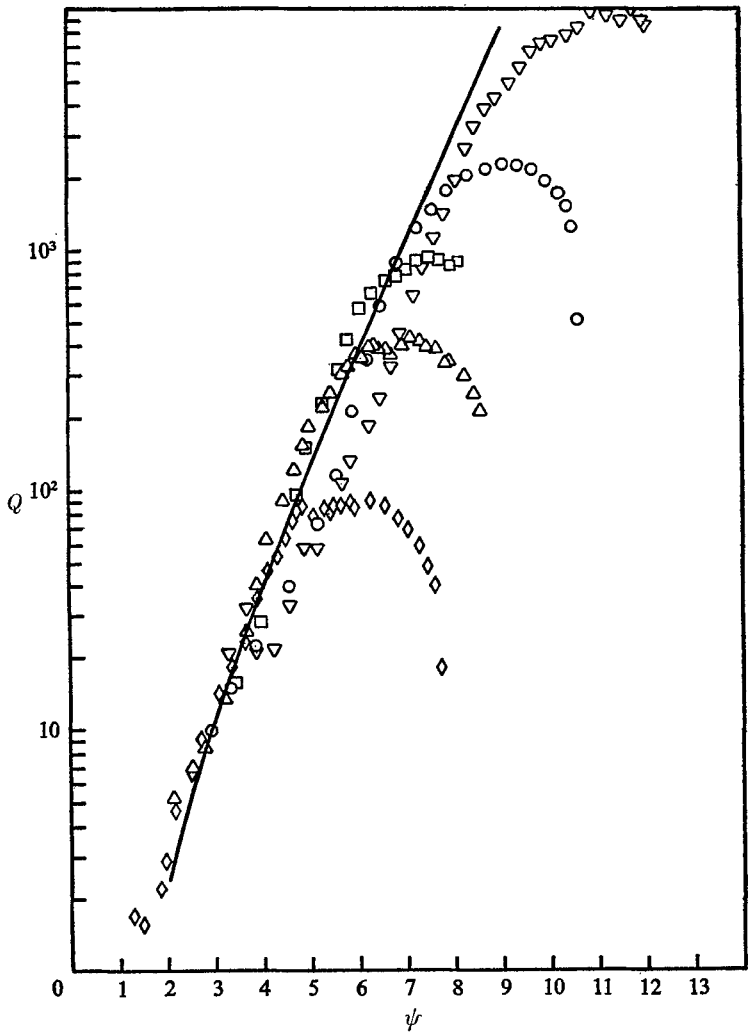

FIGURE 17. —, equation (42): constant $\dot{m}''$ flows.

	○	□	△	◇	▽
V_w/U_∞	0	0·0019	0·0038	0·0078	−0·0023
V_w^+	0	0·055	0·153	0·583	−0·043
Re_θ	3177	4301	7130	9732	1738

5.2.2. *The outer region.* The $\epsilon_M/\delta^*U_\infty$ and l/δ results from constant V_w and $V_w \propto X^{-0.2}$ turbulent flow profiles are shown on figures 20–22 for $\eta = 0{\cdot}5$. For $1000 < Re_\theta < 6000$, $l/\delta \sim Re_\theta^{-\frac{1}{8}}$ while $\epsilon_M/\delta^*U_\infty \sim Re_\theta^{-\frac{1}{4}}$. At higher Re_θ, l/δ and $\epsilon_M/\delta^*U_\infty$ are apparently functions of η only as shown in figures 23 and 24.

To verify the consistency of these ϵ_M and l results in the outer region with the velocity defect relation (24), (24) with (25) or (26) was substituted into the integrated momentum equation (44) to produce equations for $\epsilon_M/\delta^* U_\infty$ and l/δ. The resulting equations are

$$\frac{l}{\delta} = \frac{\Omega \eta S}{(1+\Pi\eta\omega')}, \tag{43}$$

and

$$\frac{\epsilon_M}{\delta^* U_\infty} = \frac{\Omega^2 S^2}{(1+\Pi\eta\omega')}\left[1 - \frac{U_\tau B f'}{2\Omega U_\infty (1+B)^{\frac{1}{2}}}\right]\left[1+\Pi+\frac{U_\tau B \int_0^1 f f''\, d\eta}{4\Omega(1+B)^{\frac{1}{2}}}\right]^{-1}, \tag{44}$$

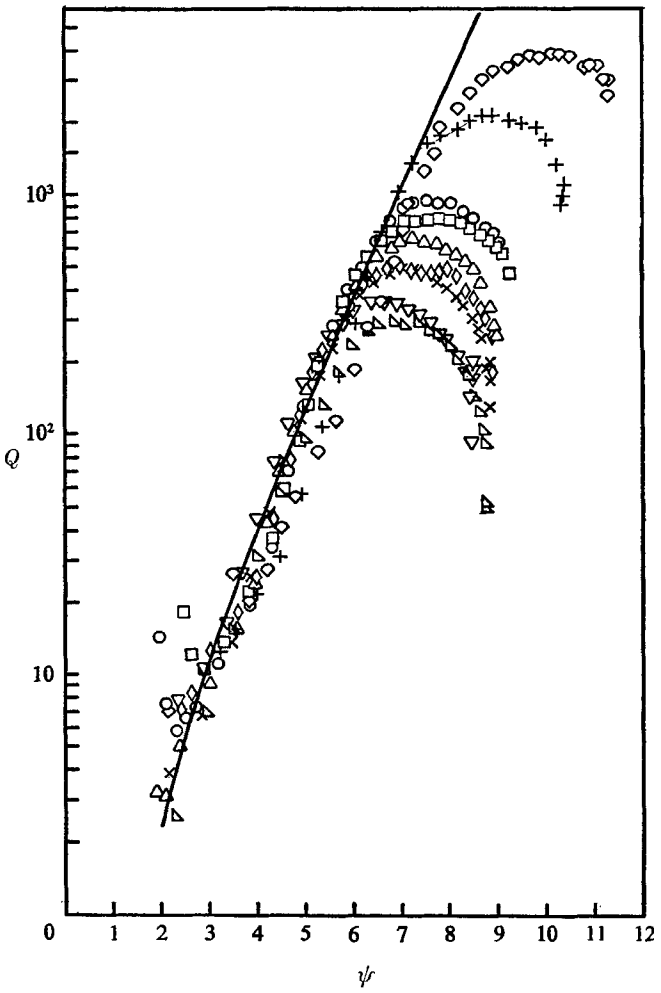

FIGURE 18. —, equation (42); constant B flows.

	□	◇	▽	○	△	×	⧋	+	▽
B	1·74	3·54	5·93	1·75	3·51	5·91	11·66	0	−0·48
V_w	0·062	0·108	0·161	0·057	0·099	0·147	0·233	0	−0·0232
Re_θ	2826	3484	4156	5344	6618	7951	9181	2238	1557

where
$$S = \left\{1 - \frac{1}{\left(1 - \frac{U_\tau B f'}{2\Omega U_\infty (1+B)^{\frac{1}{2}}}\right)^2}\left[\frac{\int_0^\eta gg''\,d\eta}{\int_0^1 gg''\,d\eta}\right]\right\}^{\frac{1}{2}},$$

$$f = -\eta \ln|\eta| + \eta + \Pi\left(2\eta - \int_0^\eta \omega\,d\eta\right),$$

and
$$g = \eta - \frac{(1+B)^{\frac{1}{2}} U_\tau f}{U_\infty \Omega} + \frac{BU_\tau^2}{4\Omega^2 U_\infty^2}\left(ff' - \int_0^\eta ff''\,d\eta\right).$$

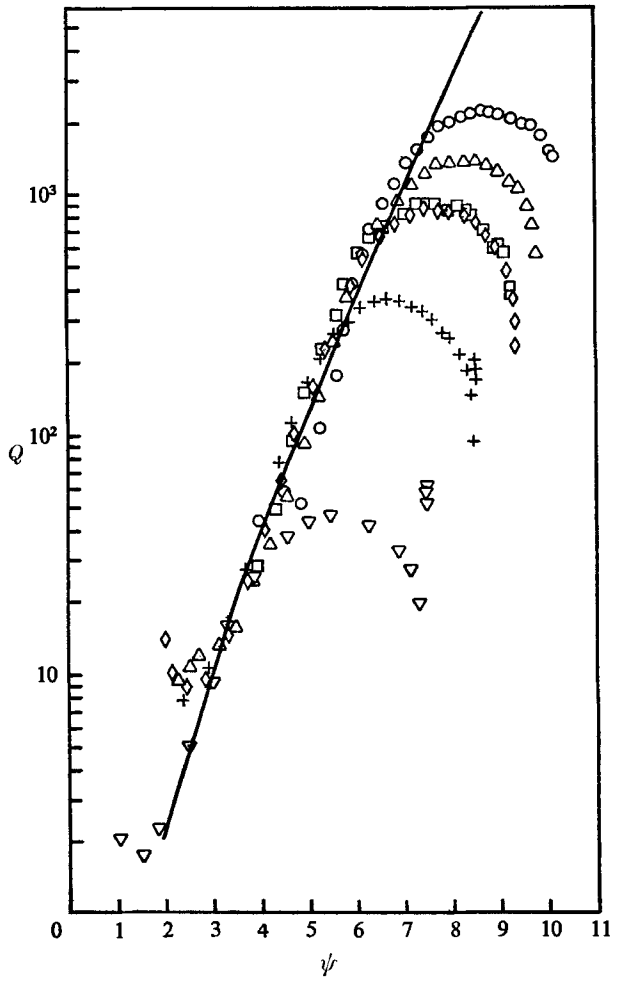

FIGURE 19. —, equation (42): approximately constant Re_θ.

	○	□	▽	△	◇	+
V_w/U_∞	0	0·0019	0·0095	—	—	—
B	—	—	—	0·72	1·79	5·93
V_w^+	0	0·055	0·727	0·026	0·059	0·161
Re_θ	4318	4301	4290	4286	4519	4156

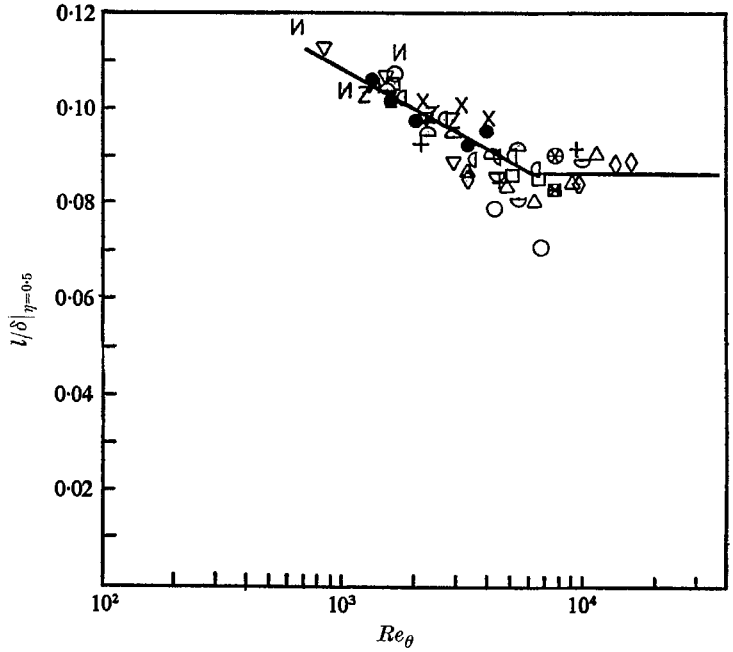

FIGURE 20. —, equation (45), $l/\delta \sim Re_\theta^{-\frac{1}{8}}$ for $Re_\theta < 6000$: constant $\dot{m}''$ and B results. Klebanoff's (1954) unblown data as presented by Escudier (1965), ∗, and Bradshaw (1967), ⊛. Data of Simpson (1967):

	$\dot{m}''/(\rho U)_\infty$			B	
×	0	○	0·0095	△	11·7
●	0·00099	Z	−0·0012	▽	−0·48
□	0·0019	N	−0·0024	⌓	0·73
+	0·0038	—		◁	1·79
◇	0·0078	—		⌔	6·78

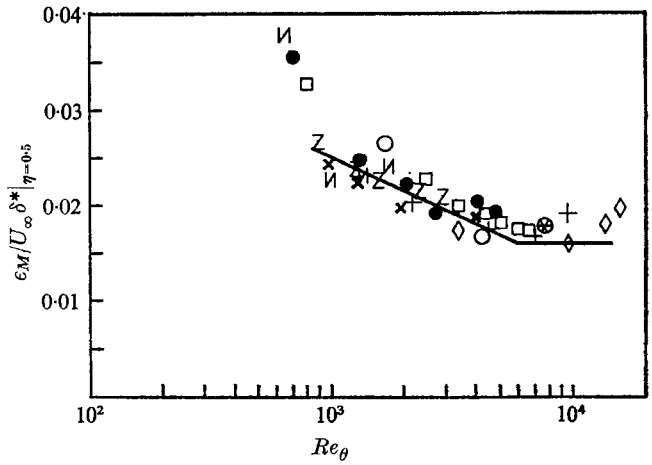

FIGURE 21. —, $\epsilon_M/U_\infty \delta^*|_{\eta=0.5} = 0{\cdot}016$, $Re_\theta \geqslant 6000$, and $\epsilon_M/U_\infty \delta^*|_{\eta=0.5} = 0{\cdot}016\, Re_\theta^{-\frac{1}{4}} \sim \Omega^2$, $Re_\theta \leqslant 6000$: constant $\dot{m}''/(\rho U)_\infty$ flows. Klebanoff's (1954) unblown data presented by Bradshaw (1967) ⊛. Data of Simpson (1967):

	×	●	□	+	◇	○	Z	N
$\dot{m}''/(\rho U)_\infty$	0	0·00099	0·0019	0·0038	0·0078	0·0095	−0·0012	−0·0024

Note that $l/\delta \sim \Omega$ and $\epsilon_M/\delta^* U_\infty \sim \Omega^2$ from these equations, a result in agreement with the generated shear stress ϵ_M and l results of figures 20–22. Results from (43) and (44) for $0 < B < 11{\cdot}92$ and $\Omega = \kappa = 0{\cdot}40$, using the experimental $(C_f/C_{f_0})_{Re_\theta}$ *vs.* B curve of figure 5 of Simpson *et al.* (1969) are shown on figures 25 and 26. The dependency of these results on B is weak, with $\epsilon_M/\delta^* U_\infty$ varying by

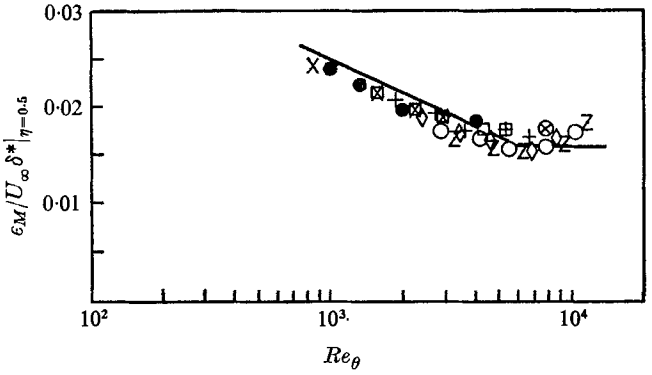

FIGURE 22. —, $\epsilon_M/U_\infty \delta^*|_{\eta=0.5} = 0{\cdot}016$, $Re_\theta \geqslant 6000$, and $\epsilon_v/U_\infty \delta^*|_{\eta=0.5} = 0{\cdot}016\, Re_\theta^{-\frac{1}{4}} \sim \Omega^2$: constant B flows. Klebanoff's (1954) unblown data presented by Bradshaw (1967), ⊗. Data of Simpson (1967):

	×	●	□	+	◇	○	Z
B	−0·48	0	0·73	1·77	3·89	6·79	11·7

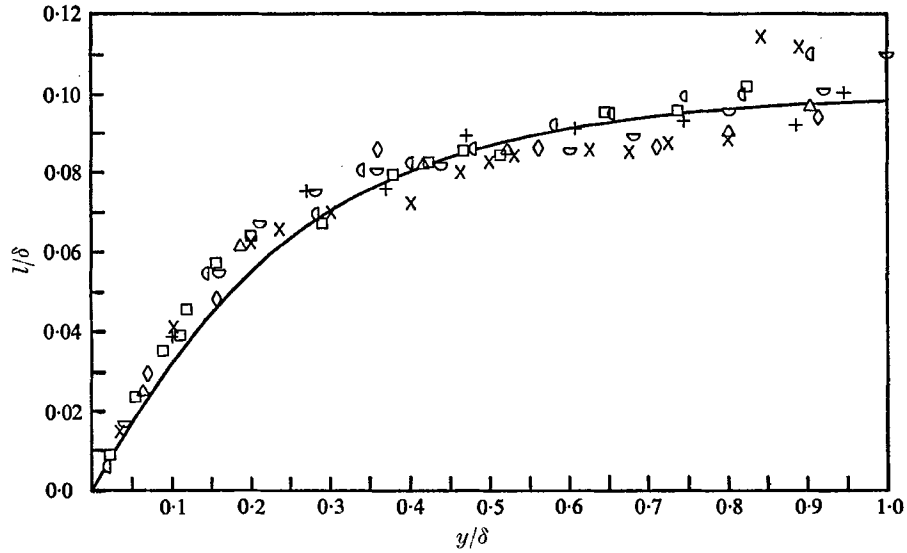

FIGURE 23. l/δ *vs.* η, $Re_\theta > 6000$. —, equation (45). Klebanoff's (1954) unblown data as presented by Escudier (1965), ×. Blown data of Simpson (1967):

	□	◇	×	+	△	◖	◡
$\dot{m}''/(\rho U_\infty)$	0·0019	0·0078	0	0·0038	—	—	—
B	—	—	—	—	11·7	11·79	6·78
Re_θ	6583	13971	7750	9429	9181	6706	7846

0·0015 between $B = 0$ and $B = 11{\cdot}7$ while l/δ varies only in the outer most region by 0·015. (This apparent weak blowing dependency in the outermost region is probably an artificality produced by the limitations of the $E(\eta, Re_\theta)$ representation as $\eta \to 1$.) These variations are within the uncertainty of the generated shear stress profile $\epsilon_M/\delta^* U_\infty$ and l/δ results, so that there is basic consistency between (24) and the generated shear stress profile $\epsilon_M/\delta^* U_\infty$ and l/δ results, i.e. (24) implies that $\epsilon_M/\delta^* U_\infty$ and l/δ are substantially independent of blowing in the outer region.

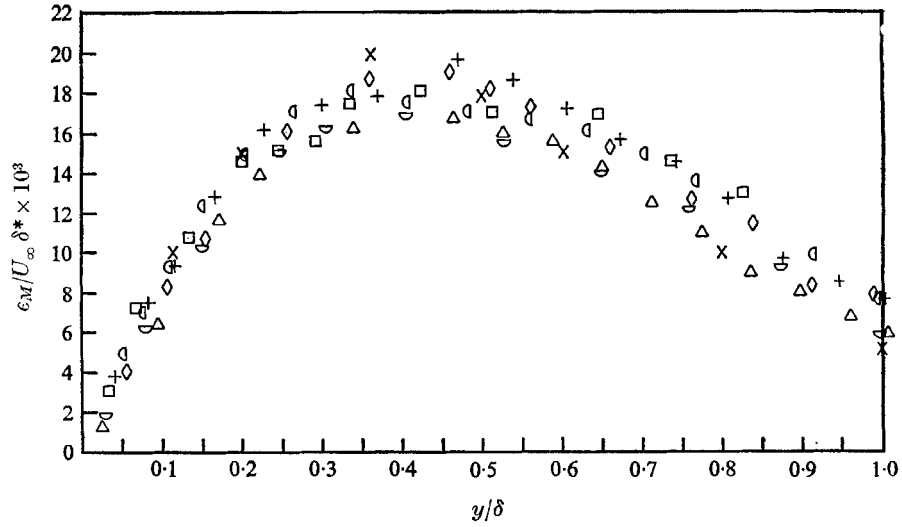

FIGURE 24. $\epsilon_M/U_\infty \delta^*$ *vs.* η, $Re_\theta > 6000$. Klebanoff's (1954) unblown data presented by Bradshaw (1967), ×. Blown data of Simpson (1967):

	□	◇	×	+	△	◁	▽
$\dot{m}''/(\rho U_\infty)$	0·0019	0·0078	0	0·0038	—	—	—
B	—	—	—	—	11·7	1·79	6·78
Re_θ	6583	13971	7750	9429	9181	6706	7846

Escudier (1965) presented l/δ results from many unblown non-zero pressure gradient flows. He presented a two-layer model with $l/\delta = \Omega\eta$ and Ω constant near the wall and constant $l/\delta = \lambda_\infty$ in the outermost region. This model fails to closely fit the l/δ results from experimental data in the vicinity of $\eta = \lambda_\infty/\Omega$ and does not provide for the variation of λ_∞ and Ω with Re_θ at low Reynolds numbers. The following single equation model for the outer region is proposed here to alleviate both problems:

$$\frac{l}{\delta} = \frac{\Omega(Re_\theta)}{4}(1 - e^{-4\eta}), \tag{45}$$

where $\Omega = 0{\cdot}40\ (Re_\theta/6000)^{-\frac{1}{8}}$ for $Re_\theta < 6000$ and $\Omega = \kappa = 0{\cdot}40$ for $Re_\theta > 6000$. As shown in figure 23, (45) closely fits Escudier's l/δ results from the Klebanoff layer and the present permeable wall results for $Re_\theta > 6000$, indicating the

acceptability of the factor containing the empirical function of η. The Ω dependence on Re_θ is likewise in agreement with the results shown on figure 20. In the limits, $l/\delta \to \frac{1}{4}\Omega$, as $\eta \to 1$, and $l/\delta \to \Omega\eta$, as $\eta \to 0$.†

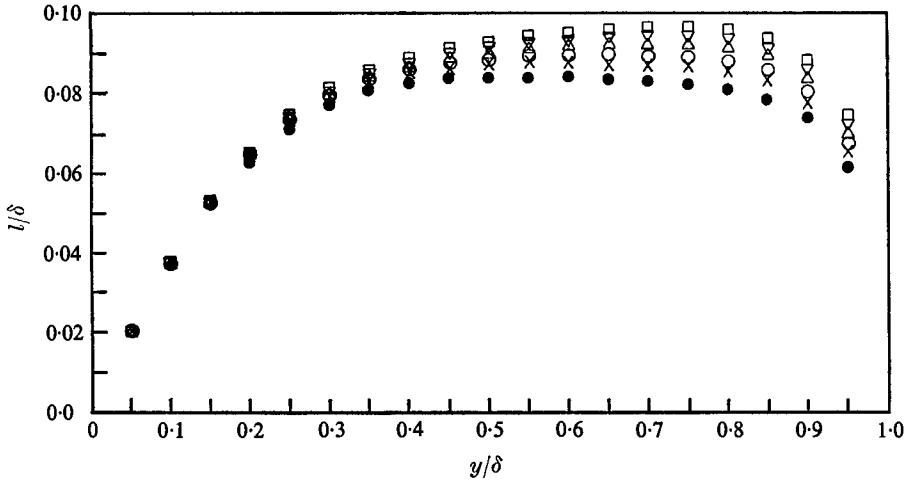

FIGURE 25. l/δ *vs.* η, $Re_\theta > 6000$, generated from the velocity defect equation, (24).

	●	×	○	△	▽	□
B	0	0·73	1·79	3·53	5·92	11·7

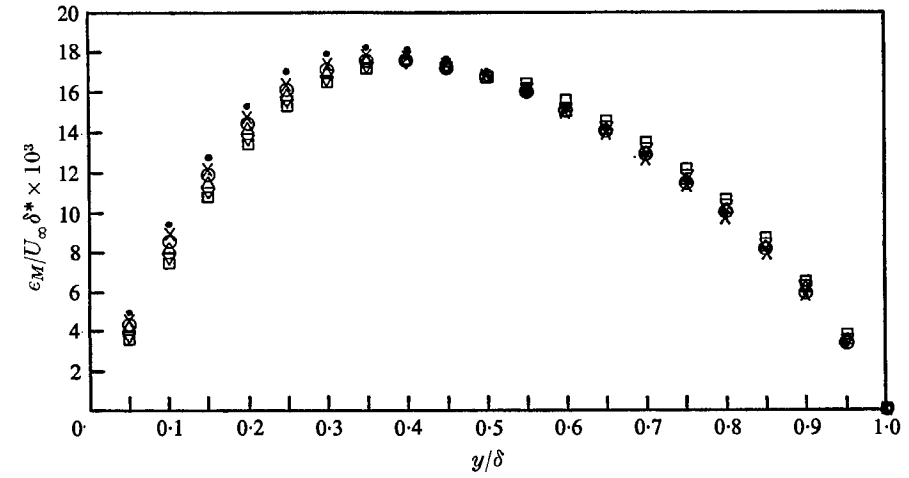

FIGURE 26. $\epsilon_M/U_\infty \delta^*$ *vs.* η, $Re_\theta > 6000$, generated from the velocity defect equation, (24).

	●	×	○	△	▽	□
B	0	0·73	1·79	3·53	5·92	11·7

† P. Bradshaw, in a private communication, indicates that the $(Re_\theta/6000)^{-\frac{1}{8}}$ factor can be also applied to the 'dissipation length' in the outer 70 % of the boundary layer for the Bradshaw *et al.* (1967) turbulence energy boundary-layer prediction method. Bradshaw *et al.* (1967) suggest that the dissipation length is independent of moderate blowing and suction. The present results support this view since the mixing length and dissipation length distributions are each universal for equilibrium boundary layers and the mixing length distribution is independent of blowing and moderate suction.

6. Discussion and conclusions

A principal conclusion from this work is that allowing Ω to vary with Re_θ for an unblown flat plate with $Re_\theta < 6000$ can account for the following:

(i) The failing of Coles's law of the wake formulation for $Re_\theta < 6000$ using a constant Ω.

(ii) The U/U_∞ *vs.* η similarity of the outer region for $Re_\theta < 6000$ in contrast to Γ *vs.* η similarity for $Re_\theta > 6000$.

(iii) The apparent $\epsilon_M/U_\infty \delta^* \sim \Omega^2$ and $l/\delta \sim \Omega$ variation of the outer region for $Re_\theta < 6000$.

Specifically, it was found that $\Omega \sim (\frac{1}{2}C_f)^{\frac{1}{2}} \sim Re_\theta^{-\frac{1}{8}}$ or U_τ/U_∞ for $Re_\theta < 6000$ was sufficient for Coles's law of the wall–law of the wake formulation to hold and obey the U/U_∞ *vs.* η similarity of the outer region for this Reynolds number range.

Several investigators have reported constant values of Ω as high as 0·47 and as low as 0·39 for unblown flat plate flows (Simpson 1967). Black & Sarnecki (1958) attempted to resolve this conflict by examining a source of discrepancy in the experimental determination of Ω, the problem of determining the 'true' value of skin friction. They attempted to adjust the values of Ω, C, and U_τ given by various investigators such that $U^+ = 16{\cdot}4$, $y^+ = 100$ with unchanged U/U_∞ *vs.* yU_∞/ν curves. This procedure did not yield universal values for Ω and C. As pointed out by Simpson (1967), a second source of discrepancy lies in the choice of the 'best' straight line through a set of experimental data points. Certainly, a third source of discrepancy is the use of different 'corrections' to the velocity profile data. A fourth source is pecularities of each different apparatus.

Until now the variation of Ω with Re_θ for $Re_\theta < 6000$ has not been recognized. Hence, this variation of Ω with Re_θ may account for some of the reported discrepancy of Ω among various investigations. For example, an investigator may obtain zero injection data for $1000 < Re_\theta < 6000$ and fit a constant value of Ω through these data, obtaining a value between 0·5 and 0·4. In particular, Black & Sarnecki (1958) report a constant $\Omega = 0{\cdot}45$ for their zero injection experiments with $1000 < Re_\theta < 3500$.

It was found that for blown and undersucked flows ($d\theta/dX > 0$) $\Omega(Re_\theta)$, $E(\eta, \Pi, Re_\theta)$ of the velocity defect representation, and l/δ and $\epsilon_M/U_\infty\delta^*$ of the outer region are substantially independent of transpiration. On the other hand, the 'law of the wall' velocity and ϵ_M/ν distributions near the wall and the velocity-defect variable Γ are strong functions of transpiration.

As was pointed out, the 'law of the wall' correlation is strongly dependent upon the experimental $\frac{1}{2}C_f$ values obtained. Thus, if we accept the $\frac{1}{2}C_f$ results of Simpson (1967) as reasonable values supported by the results of other investigators, then (22) serves as a 'law of the wall for injection and undersucked layers' with variable Ω. Likewise, the variables Q and Ψ from (42), which incorporates (22), serve to correlate the blowing ϵ_M/ν results near the wall.

Several problems were more closely defined in conjunction with this study:

(i) Very little subsonic injection data and undersucked data exist for $Re_\theta > 6000$, the range for most applications.

(ii) As $\frac{1}{2}C_f$ approaches zero for injection flows, more accurate experimental

$\frac{1}{2}C_f$ values are needed to further verify (22) as a 'law of the wall with injection'. Commonly used techniques will probably not provide this information. As was pointed out, $\frac{1}{2}C_f$ determined from the momentum integral technique is highly uncertain for large injection. Any technique using a probe near the wall to measure a velocity profile runs the risk of highly disturbing the flow since $\partial U/\partial y$ approaches zero as U approaches zero. Hence, in future efforts to measure extremely small $\frac{1}{2}C_f$ values, a technique not disturbing the wall flow should be used.

(iii) As discussed above, some investigators attribute the discrepancy of the high blowing $\frac{1}{2}C_f$ values from different apparatus to differences in surface roughness and injection geometry. Since no experimental investigation of these effects has been made to date, it is difficult to access the relative importance of these effects at high blowing.

The author is grateful for the encouragement of Professors W. M. Kays and R. J. Moffat of Stanford University during the preparation of this work. He thanks the Institute of Technology, Southern Methodist University, for financial aid.

REFERENCES

BLACK, T. J. & SARNECKI, A. J. 1958 *Aero. Res. Counc. Rep.* 20, 501, F.M. 2745; also 1965 *Aero. Res. Counc. R & M* 3387.

BRADSHAW, P. 1967 *J. Fluid Mech.* **29**, 625.

BRADSHAW, P., FERRISS, D. H. & ATWELL, D. A. 1967 *J. Fluid Mech.* **28**, 593.

CLARK, J. H., MENKES, H. R. & LIBBY, P. A. 1955 *J. Aero. Sci.* **22**, 255.

COLES, D. 1956 *J. Fluid Mech.* **1**, 191.

COLES, D. 1962 *Rand Rep.* R-403-PR.

DAHM, T. J. & KENDALL, R. M. 1968 *AIAA J.* **6**, 1822.

DERSHIN, H., LEONARD, C. A. & GALLAHER, W. A. 1967 *AIAA J.* **5**, 1934.

DORRANCE, W. J. & DORE, F. J. 1954 *J. Aero. Sci.* **21**, 104.

ESCUDIER, M. P. 1965 *Imperial College. Mech. Engrg. Rep.*, TWF/TN/1.

FAVRE, A., DUMAS, R., VEROLLET, E. & COANTIC, M. 1966 *J. de Mécanique* **5**, 3.

FRASER, M. D. 1964 Sc.D. Thesis, MIT.

HINZE, J. O. 1959 *Turbulence.* New York: McGraw-Hill.

KENDALL, R. M. 1959 Sc.D. Thesis, MIT.

KENDALL, R. M., RUBESIN, M. W., DAHM, T. J. & MENDENHALL, M. R. 1964 *Vidya, Palo Alto, Calif., Vidya Rep.* 111 (AD 69 209).

KINNEY, R. B. 1967 *AIAA J.* **5**, 624.

KLEBANOFF, P. S. 1954 *NACA TN* 3178.

KLEINSTEIN, G. 1967 *AIAA J.* **5**, 1402.

KLINE, S. J. 1965 *Proc. Inst. Mech. Engrs.* **180**, 222.

KLINE, S. J., COCKRELL, D. J. & MORKOVIN, M. V. (ed). 1968 *Proc.* 1968 *Conf. on Turbulent Boundary Layer Prediction.* **1**.

MCQUAID, J. 1966 Ph.D. Thesis, Cambridge University.

MICKLEY, H. S. & DAVIS, R. S. 1957 *NACA TN* 4017.

MICKLEY, H. S., ROSS, R. C., SQUYERS, A. L. & STEWART, W. E. 1954 *NACA TN* 3208.

MICKLEY, H. S. & SMITH, K. A. 1963 *AIAA J.* **1**, 1685.

MICKLEY, H. S., SMITH, K. A. & FRASER, M. D. 1964 *AIAA J.* **2**, 173.

MICKLEY, H. S., SMITH, K. A. & FRASER, M. D. 1965 *AIAA J.* **3**, 787.

MOFFAT, R. J. & KAYS, W. M. 1967 *Stanford University, Mech. Engrg. Rep.* HMT-1; also 1968 *Int. J. Heat Mass Trans.* **11**, 1547.

ROTTA, J. C. 1962 *Progress in Aero. Sciences*, **2**, 1. New York: MacMillan.

ROTTA, J. C. 1966 *Deutsche Luft und Raumfahrt Forsch. ber.* **6**, 45.

RUBESIN, M. W. 1954 *NACA TN* 3341.

SCHUBAUER, G. G. 1954 *J. Appl. Phys.* **25**, 188.

SIMPSON, R. L. 1967 Ph.D. Thesis, Stanford University; available from University Microfilms, Ann Arbor, Mich.

SIMPSON, R. L., MOFFAT, R. J. & KAYS, W. M. 1969 *Int. J. Heat Mass Trans.* **12**, 771.

SIMPSON, R. L. & WHITTEN, D. G. 1968 *AIAA J.* **6**, 1776.

SIMPSON, R. L., WHITTEN, D. G. & MOFFAT, R. J. 1970 *Int. J. Heat Mass Trans.* **13**, 125.

SMITH, K. A. 1962 Sc.D. Thesis, MIT.

SPALDING, D. B. 1961 *TASME J. Appl. Mech.* **28**, 455.

STEVENSON, T. N. 1963*a* *Cranfield Coll. of Aero., Aero. Rep.* 166.

STEVENSON, T. N. 1963*b* *Cranfield Coll. of Aero., Aero. Rep.* 170.

STEVENSON, T. N. 1964 *Cranfield Coll. of Aero., Aero. Rep.* 177.

STEVENSON, T. N. 1968 *AIAA J.* **6**, 553.

TORII, K., NISHIWAKI, N. & HIRATA, M. 1966 *Proc. Third Inter. Heat Transfer Conf.* **3**, 34.

WHITTEN, D. G. 1967 Ph.D. Thesis, Stanford University; available from University Microfilms. Ann Arbor, Mich.

WHITTEN, D. G., KAYS, W. M. & MOFFAT, R. J. 1970 *Int. J. Heat Mass Trans.* (To be published.)

WIEGHARDT, K. 1943 *Göettingen U & M Rept.* 6603.

WOOLDRIDGE, C. E. & MUZZY, R. J. 1966 *AIAA J.* **11**, 2009.